A METHOD OF IODINE DETERMINATION BY CHARACTERISTIC X-RAY ABSORPTION

by

Orest Z. Roy, B.Sc. E.E.

A thesis submitted to the Faculty of Graduate Studies and Research in partial fulfilment of the requirements for the degree of Master of Engineering.

Research Director - Dr. G. L. d'Ombrain

Associate Director - Dr. R. A. Beique

Department of Electrical Engineering,
McGill University,
Montreal.

August 1960

ACKNOWLEDGEMENTS

The author would like to express his thanks to the James Picker Foundation for their financial assistance and to the National Research Council for a leave of absence, in particular to Dr. D.W.R. McKinley and Mr. C.F. Pattenson of the Radio and Electrical Engineering Division. Also sincere thanks are extended to the staff of the Radiology Department of the Montreal General Hospital, in particular to Dr. R. A. Beique for his advice and encouragement and to Mr. R.W. Rolf whose mechanical abilities were greatly appreciated.

ABSTRACT

This thesis describes a simple technique for the quantitative in vivo analysis of nonradioactive iodine. The method uses the X-ray absorption discontinuities for the detection of iodine in the presence of any other absorbing substance.

A stationary lanthanum radiator converts an X-ray beam having a continuous spectrum into two monochromatic beams which straddle the iodine absorption edge. The energy spread is such as to make the technique relatively independent of other foreign elements. A rotating filter alternately selects one of the two beams and a switch synchronously channels these separated beams into two counting circuits.

The intensity of the beams is measured by two counting rate meters and the ratio of these intensities is obtained by a conventional self-balancing potentiometer. Since this ratio is determined every 1/120 of a second the iodine determination is insensitive to X-ray output, amplifier and detector drift. Throughout the entire electronic system standard circuits are used with standard tolerance components. This simple technique appears to be reliable, drift free and less complex than previous methods.

TABLE OF CONTENTS

LIST OF TABLES

LIST OF ILLUSTRATIONS

INTRODUCTION

In recent years much emphasis has been placed on methods for the elimination of all unnecessary radiation whether it be caused by atomic fall-out or in the diagnostic procedures involving standard X-ray techniques. All radiation may be harmful to humans, however, in many instances radiation is mandatory. For this reason extensive investigations are being carried out in an effort to optimize the information obtained in these instances.

The purpose of this investigation is to develop a technique and instrumentation for the quantitative analysis of heavy elements such as iodine, through the use of monochromatic roentgen radiation. Many diagnostic procedures use radioactive heavy elements to determine some body function, such as thyroid up-take. The measurement is usually over in a matter of minutes while the radioactivity lasts for weeks, thus producing a great deal of unnecessary radiation. It is hoped that with the monochromatic radiation technique some of this unnecessary radiation will be eliminated.

Much of the pioneer work in the field of iodine determination has been done by B. Jacobson at the Karolinska Institutet in Stockholm, Sweden, and liberal reference to this work is made in the text. It is felt that this new system to be described is simpler and more sensitive for nonradioactive iodine determination than the previous methods.

A complete theoretical analysis of this new method will be made as well as a detailed description of the instrumentation and techniques involved. Results will be stated and suggestions for improvement made.

CHAPTER I

THEORY

FUNDAMENTAL PRINCIPIES

The amount of X-ray energy absorbed is determined by the energy of the radiation, the thickness and the elementary composition of the absorbing layers. The intensities I(o) and I of the incident and transmitted rays are related by

$$I = I(o) \exp -(U_1x_1 + U_2x_2 ++) \qquad 1.1$$

Where U_n is the attenuation coefficient of the elements n in the absorbing layer and x_n the corresponding mass. The attenuation coefficients for an element depend on the energy of the radiation and on the absorbing substance. In general the attenuation decreases with energy but at certain energies absorption discontinuities or edges occur. The discovery that the attenuation curve as a function of energy contains discontinuities was made by M. deBroglie in 1916. Because of these attenuation edges which are characteristic of each individual element a method of detection and analysis through the use of monochromatic radiation is made possible.

PRODUCTION OF MONOCHROMATIC RADIATION

Monochromatic X-rays are produced by secondary radiation. When a polychromatic beam is allowed to bombard a radiator, two distinct types of secondary X-radiation are obtained. One is known as unmodified radiation and is almost identical to the primary beam. The second is

fluorescent radiation, which is less penetrating or of lower energy than the primary beam. Unmodified radiation seems to be primary rays which have had their direction slightly altered without much energy change. Whereas fluorescent radiation is characteristic of the radiator and does not change in character with change in energy of the primary beam as long as this beam is of sufficient energy to excite fluorescences. Fluorescence radiation is the ionization and subsequent recombination of the atoms of the radiator. When X-rays traverse matter part of their energy is spent in ejecting beta rays or electrons from some of the atoms. The remainder of the atom is in an ionized condition and as it regains its normal state, energy is liberated which reappears as fluorescence X-rays.

Table 1 gives the fluorescent radiation energies of a few elements as well as their attenuation edges (Fine and Hendee 1955).

BASIC THEORY

By measuring the variation in attenuation of two energies E_1 and E_2 lying close to but on opposite sides of the attenuation edge of a certain element, its concentration can be determined.

From figures 1 and 2 and using equation 1.1 we see that

$$I_1 = I_{01} \exp -(U_{11}x_1 + U_{21}x_2) \qquad 1.2$$

$$I_2 = I_{02} \exp -(U_{12}x_1 + U_{22}x_2) \qquad 1.3$$

where U_{11} is the attenuation coefficient of element 1 for X-ray beam 1.

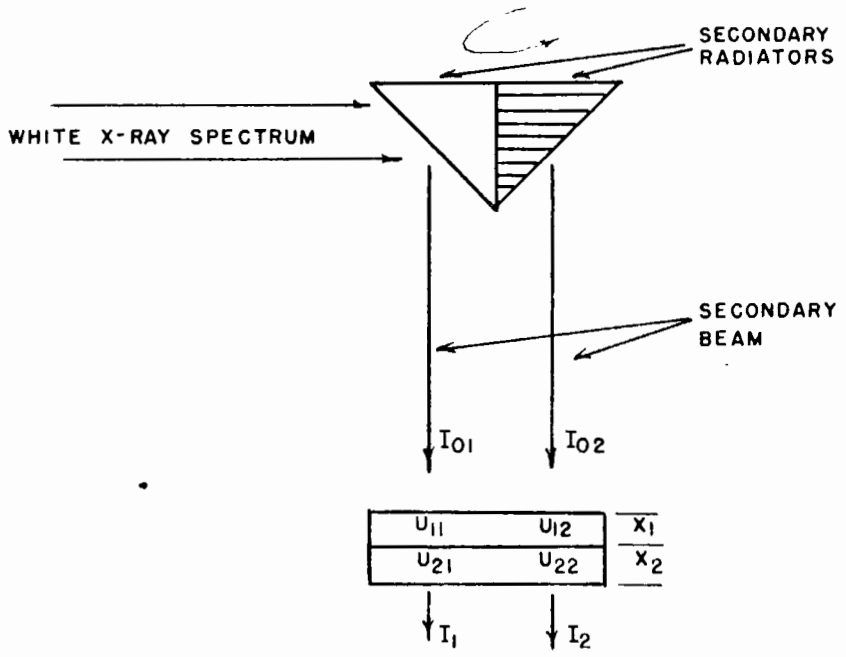

FIG. 1 SCHEMATIC EXPERIMENTAL SETUP

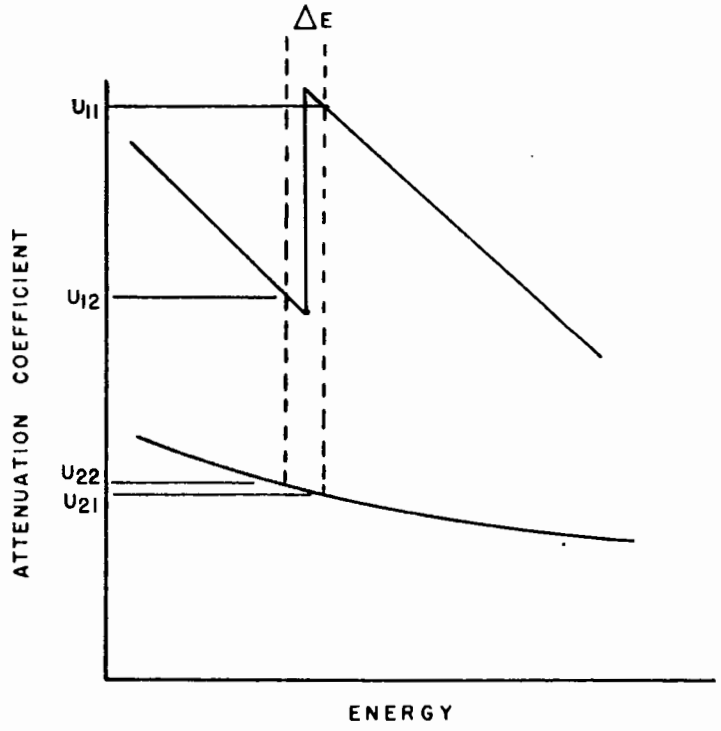

FIG. 2 SCHEMATIC ATTENUATION CURVE

TABLE I

CRITICAL ABSORPTION AND EMISSION ENERGIES

Atomic Number	Element	Absorption Kev Edge K_{ab}	Emission Energies Kev K_{a1}	K_{a2}
53	Iodine	33.164	28.610	28.315
55	Cesium	35.959	30.970	30.623
56	Barium	37.410	32.191	31.815
57	Lanthanum	38.931	33.440	33.033
58	Cerium	40.449	34.717	34.276

U_{21} is the attenuation coefficient of element 2 for X-ray beam 1.

U_{12} is the attenuation coefficient of element 1 to X-ray beam 2.

U_{22} is the attenuation coefficient of element 2 to X-ray beam 2.

x_1 is the mass of element 1.

x_2 is the mass of element 2.

Taking the ratio of equations 1.2 and 1.3

$$\frac{I_1}{I_2} = \frac{I_{01}}{I_{02}} \exp -(U_{11} - U_{12})x_1 \exp -(U_{21} - U_{22})x_2 \qquad 1.4$$

From equation 1.4 we see that in order to detect an element x_1, which has an absorption edge, in the presence of other foreign elements, the difference in the first exponent $U_{11} - U_{12}$ should be as large as possible while the difference in the second exponent $U_{21} - U_{22}$ should be as small as possible. This indicates that the spread in energy across the absorption edge should be as small as possible, in other words just straddling the absorption edge. With this condition the $U_{21} - U_{22}$ term can be neglected.

$$\text{Hence } x_1 = \frac{1}{U_{11} - U_{12}} \ln \frac{I_2 A}{I_1} \qquad 1.5$$

$$\text{where } A = \frac{I_{01}}{I_{02}}$$

Thus equation 1.5 shows that iodine concentration x_1 can be determined and is completely independent of any foreign elements. Taking the sum or difference of equations 1.2 and 1.3 produces an impractical result. The method described above was first proposed in 1925 by Glocker and Frohnmayer then by Engstrom (1946) and Jacobson (1953, 1958).

The last author uses two secondary radiators, iodine and cerium, for the production of monochromatic radiation. These radiators are cyclically alternated in the X-ray beam and thus produce monochromatic radiation of two distinct wave lengths, one on either side of the iodine absorption edge and in serial form.

The lanthanum system which is to be described uses a single, stationary, lanthanum radiator. As shown in Table I lanthanum produces two secondary beams one on either side of the iodine absorption edge. The spread in energy between the two beams K_{a1} and K_{a2} is a minimum, hence, the use of lanthanum as a converter gives the most sensitive method for iodine determination with the least dependence on foreign elements. However, the use of a single stationary filter creates a problem in that both monochromatic beams are present in parallel fashion, whereas it is necessary to have them in serial form. To overcome this difficulty an arrangement analogus to a low pass filter is utilized. An iodine filter which allows the low energy K_{a2} beam to pass while absorbing the high energy beam is periodically introduced into the secondary beam. Thus for a period of time we first have the low energy beam and then the sum of both the low and high energy beams.

In order to have the intensities of the single beam and the sum of the two beams equal, thus eliminating the unmodified scatter and probe saturation (discussed later), a second filter segment containing barium is used to attenuate the sum of the two energies.

LANTHANUM SYSTEM THEORY

The following is a mathematical analysis of the lanthanum system. Figures 3A and 3B show the two conditions of the lanthanum system, neglecting foreign elements.

From fig. 3A $I'_1 = I_{a1} \exp -(U_{1B}x_B)$

$I'_2 = I_{a2} \exp -(U_{2B}x_B)$

$I''_1 = I'_1 \exp -(U_1x_1)$

$I''_2 = I'_2 \exp -(U_2x_1)$

let $I_B = I''_1 + I''_2$

$$\text{then } \frac{I_B}{I_{a1}} = \exp -(U_{1B}x_B + U_1x_1) + \frac{I_{a2}}{I_{a1}} \exp -(U_{2B}x_B + U_2x_1) \qquad 1.6$$

Similarly from fig. 3B. let $I_I = I''_1 + I''_2$

$$\frac{I_I}{I_{a1}} = \exp -(U_{1I}x_I + U_1x_1) + \frac{I_{a2}}{I_{a1}} \exp -(U_{2I}x_I + U_2x_1) \qquad 1.7$$

Taking the ratio of 1.6 and 1.7 we get

$$f(x) = \frac{I_B}{I_I} = \frac{\exp -(U_{1B}x_B + U_1x_1) + K \exp -(U_{2B}x_B + U_2x_1)}{\exp -(U_{1I}x_I + U_1x_1) + K \exp -(U_{2I}x_I + U_2x_1)}$$

where $K = \frac{I_{a2}}{I_{a1}}$

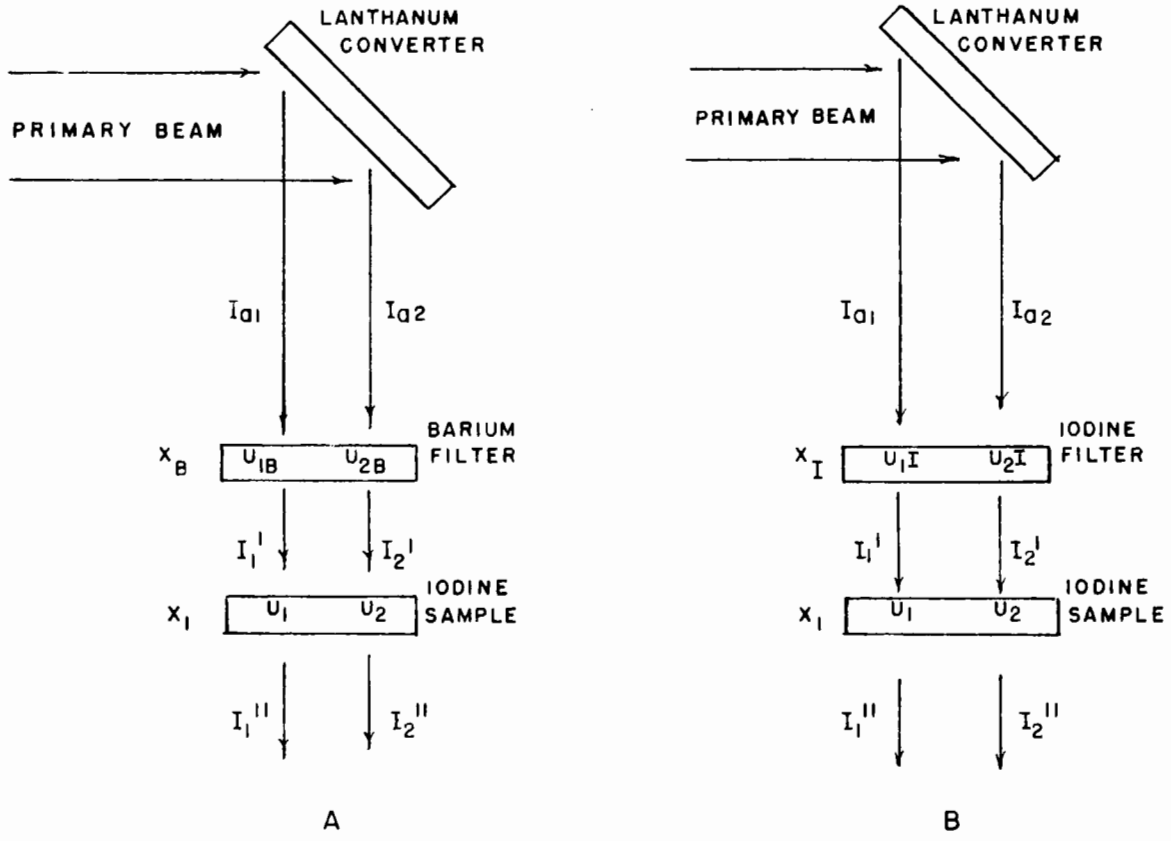

FIG. 3 LANTHANUM SYSTEM

and U_{1B}, U_{2B} are the attenuation coefficients of the barium filter

U_1, U_2 are the attenuation coefficients of the iodine sample

U_{1I}, U_{2I} are the attenuation coefficients of the iodine filter

x_B is the mass of the barium filter

x_1 is the mass of the iodine sample

x_I is the mass of the iodine filter

Since we are interested in extremely small values of x_1 we will use Maclaurin's expansion about $x_1 = 0$ normalized to unity when $x = 0$.

$$f(x) = \frac{f(0)}{f(0)} + \frac{x\, f'(0)}{f(0)} + \frac{x^2 f''(0)}{\lfloor 2\, f(0)} + \quad + \quad +$$

where f(0), f'(0), f''(0) --- are the zero, first, second etc. derivatives of f(x) evaluated at x = 0.

$$f(0) = \frac{\exp -(U_{1B}x_B) + K \exp -(U_{2B}x_B)}{\exp -(U_{1I}x_I) + K \exp -(U_{2I}x_I)}$$

$$\frac{f'(0)}{f(0)} = \frac{-K(U_1-U_2)\exp-(U_{1B}x_B+U_{2I}x_I)+K(U_1-U_2)\exp-(U_{2B}x_B+U_{1I}x_I)}{\exp-(U_{1B}x_B+U_{1I}x_I)+K\exp-(U_{1B}x_B+U_{2I}x_I)+K\exp-(U_{2B}x_B+U_{1I}x_I)+ K^2\exp-(U_{2B}x_B+U_{2I}x_I)}$$

The orders of magnitude of the parameters are $U_{1I} = 30$

$U_{2I} = 4$ (Compton 1957

$K = 0.5$ p. 640)

and $U_{1B} \cong U_{2B}$

Therefore with the proper choice of x_I any term with exp - $(U_{1I}x_I)$ can be made negligible compared to exp $-(U_{2I}x_I)$.

$$\text{Therefore } \frac{f'(0)}{f(0)} = \frac{-(U_1 - U_2)}{1 + K} .$$

Then the first two terms of the Maclaurin series are

$$f(x)=f(0)\left[1 + \frac{f'(0)}{f(0)} x_1\right]$$

$$= \frac{1 + K}{K}\left[\exp -(U_{1B}x_B - U_{2I}x_I)\right]\left[1 - \frac{(U_1-U_2)}{1+K} x_1\right] \qquad 1.8$$

now we see that the slope or sensitivity term is $-\frac{(U_1 - U_2)}{1 + K}$.

Substituting for $(U_1 - U_2)$ and K with the values given previously the slope is found to be 0.017 units per milligram of iodine.

Furthermore, if the transmission through the filter segments is made equal, i.e. $U_{1B}x_B = U_{2I}x_I$

$$\text{then } f(x) = \frac{1 + K}{K}\left[1 - \frac{(U_1 - U_2)}{1 + K} x_1\right] \qquad 1.9$$

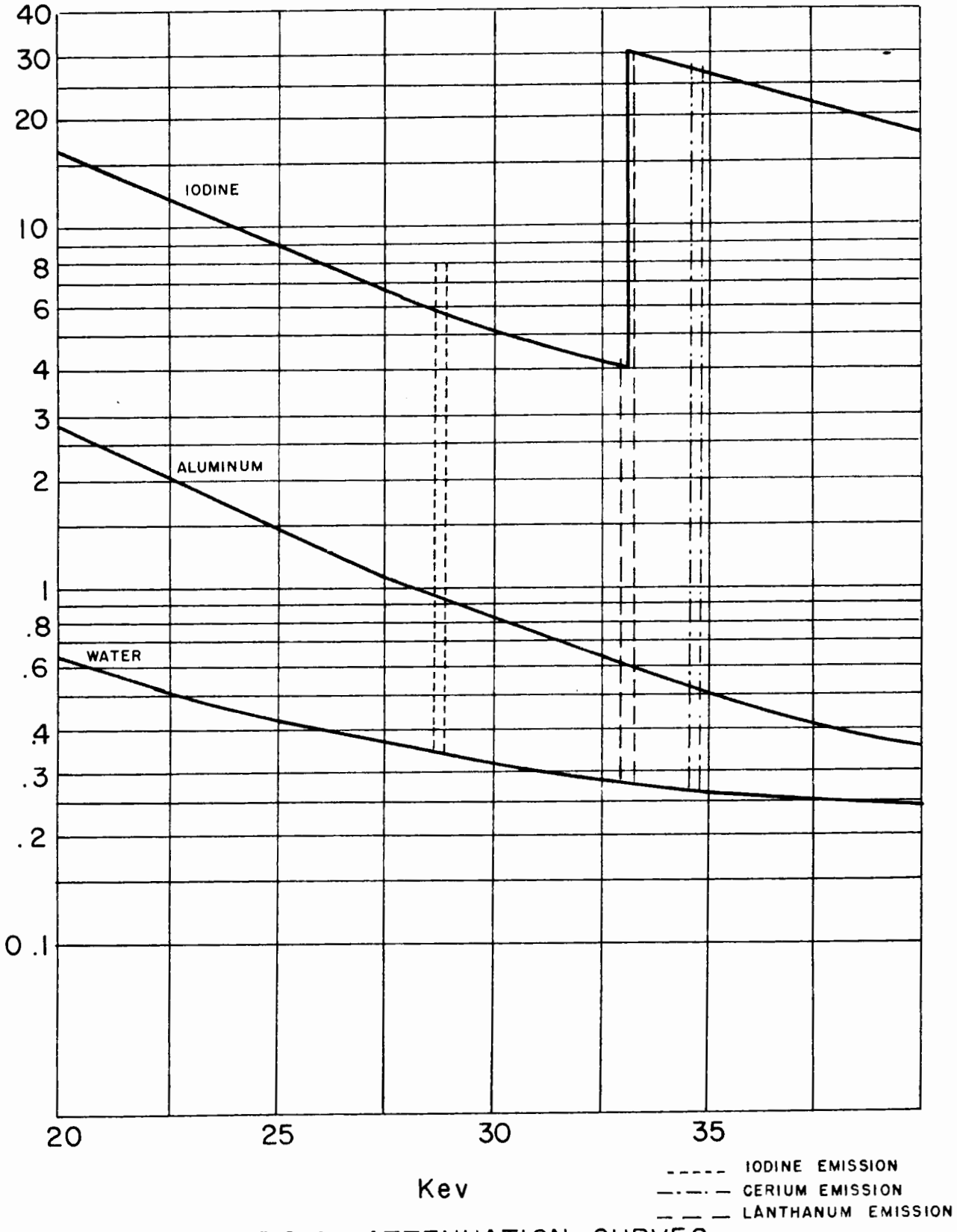

FIG. 4 ATTENUATION CURVES

COMPARISON OF THE CERIUM-IODINE AND LANTHANUM SYSTEMS

The two systems will be compared by showing the effect of bone and soft tissue on iodine determination and the sensitivity of each system to small quantities of iodine.

Throughout the comparison, aluminum will be taken as an analog to bone while water will be the analog of soft tissue.

As stated previously the energy spread between the two monochromatic rays should be as small as possible to give best sensitivity and least interaction by foreign elements.

Energy spread of the cerium-iodine system is

from Table I. $dE = 34.717 - 28.610$

$= 6.11$ Kev.

Lanthanum energy spread is $dE = 33.440 - 33.033$

$= 0.41$ Kev.

From figure 4 the attenuation coefficient of aluminum at 33.164 Kev is 0.6 cm^2/gm.

Attenuation coefficient of water is 0.27 cm^2/gm.

It is now necessary to find the change in attenuation coefficient for both aluminum and water caused by the energy spread shown above. Where we have a large energy spread the values of attenuation coefficients can be read directly from figure 4. However, in the case of small energy spreads we must resort to a theoretical calculation. Evans has shown that the attenuation coefficient $U = \frac{K}{E^3}$ (Evans 1955, p.698)

where K is a constant

E is energy Kev

U is the attenuation cm^2/gm

$$\ln U = \ln K - 3 \ln E$$

$$\frac{dU}{U} = -3 \frac{dE}{E}$$

Thus the change in attenuation coefficient for aluminum using the cerium-iodine system is

$$dU = 0.39 \ cm^2/gm.$$

The change in attenuation coefficient for water is

$$dU = 0.15 \ cm^2/gm.$$

For the Lanthanum system the change is

Aluminum -- $dU = 0.026 \ cm^2/gm$

Water -- $dU = 0.010 \ cm^2/gm.$

From equation 1.4 we see that

$$f(x) = A(\exp -dU_1x_1 \exp -dU_2x_2)$$

where dU_1 is the change in attenuation coefficient across the absorption edge of iodine

dU_2 is the change in attenuation coefficient of the foreign element, e.g. aluminum, water.

x_1 is the quantity of iodine

x_2 is the quantity of foreign element

We can now compare the two systems showing the effect of foreign matter on iodine determination.

From equation 1.4 by equating the two exponential terms we can derive the relationship

$$\frac{x_2}{x_1} = \frac{dU_1}{dU_2}$$

For the cerium-iodine system the change in attenuation coefficient across the discontinuity is

$$dU_1 = 26 - 6$$

$$= 20 \text{ cm}^2/\text{gm} \text{ from figure 4}$$

therefore $\frac{x_2}{x_1} = 50$ for aluminum

i.e. 50 grams of aluminum produce the same effect on the ratio f(x) as 1 gram of iodine,

and $\frac{x_2}{x_1} = 130$ for water.

For the lanthanum system the change in attenuation coefficient across the discontinuity is

$$dU_1 = 30 - 4$$

$$= 26 \text{ cm}^2/\text{gm} \text{ from figure 4}$$

therefore $\frac{x_2}{x_1} = 1000$ for aluminum

and $\frac{x_2}{x_1} = 2600$ for water.

The iodine detection sensitivities of the two systems can be compared by deriving the slope term for the cerium-iodine system. Using the same procedure as that shown for the derivation of equation 1.9,

the result is

$$f(x) = A(1 - dU_2x_1).$$

Thus the slope term is 0.02/milligram of iodine, whereas for the lanthanum system it is 0.017/milligram of iodine.

The above results can be best summarized in table form.

TABLE II

COMPARISON OF THE CERIUM-IODINE AND LANTHANUM SYSTEMS

Milligrams of foreign matter having the same effect on f(x) as 1 milligram of iodine	Lanthanum System	Cerium-Iodine System
Bone	1000	50
Soft Tissue	2600	130
Slope (milligram of iodine)$^{-1}$	0.017	0.02

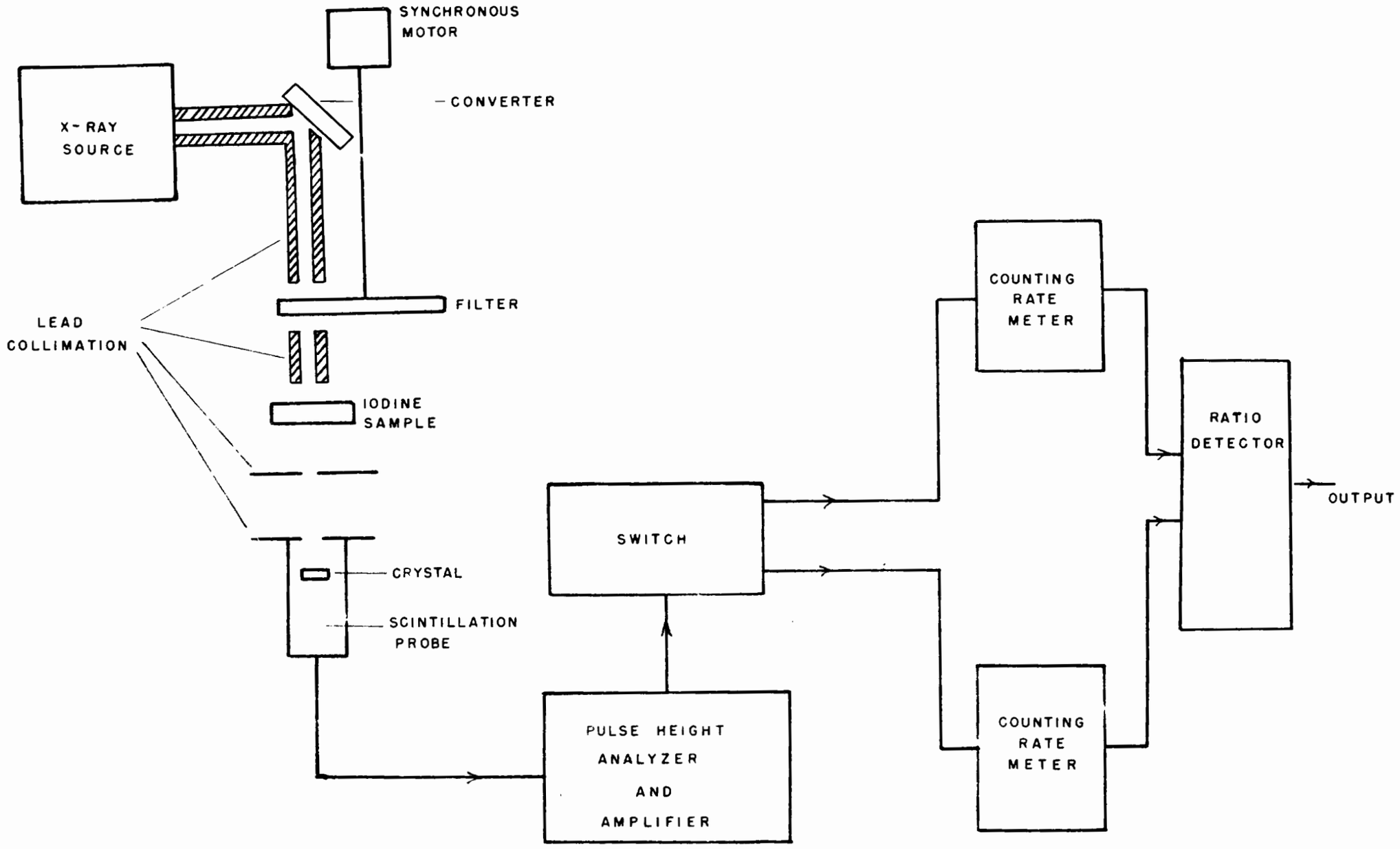

FIG. 5 SYSTEM BLOCK DIAGRAM

CHAPTER II

METHOD OF OPERATION

Figure 5 is a block diagram of the instrumentation involved in the determination of iodine.

The primary beam of X-rays is supplied by a conventional General Electric KX-11 Type 4 diagnostic X-ray unit. The machine produces a pulsating D.C. voltage, through full wave rectification, which can be varied from 30 kilovolts to 100 kilovolts with currents ranging from 0 to 10 milliamperes.

The converter is made of lanthanum chloride powder which is placed in a plastic container 1" wide, 2" long and $\frac{1}{2}$" deep. The container is situated 10 cm. from the X-ray tube target. The secondary radiation is extracted at an angle of 90 degrees to the primary beam, in this way minimizing the unmodified scatter (Nelms 1953, p. 50).

Collimation of both the primary and secondary beams is obtained by using a 2 inch diameter lead pipe containing a 3/4 inch hole. Additional collimation over the detector to improve the system geometry is provided by 1/16 inch lead sheets.

As stated in the previous chapter a filter containing two separate elements is necessary. One of these, iodine, absorbs the high energy beam I_{a1} of lanthanum, the other, barium, absorbs both the I_{a1} and I_{a2} beams equally. When the iodine segment is in the beam complete elimination of the I_{a1} beam is impossible. It was found empirically that an iodine concentration of 200 milligrams/cm^2 elimi-

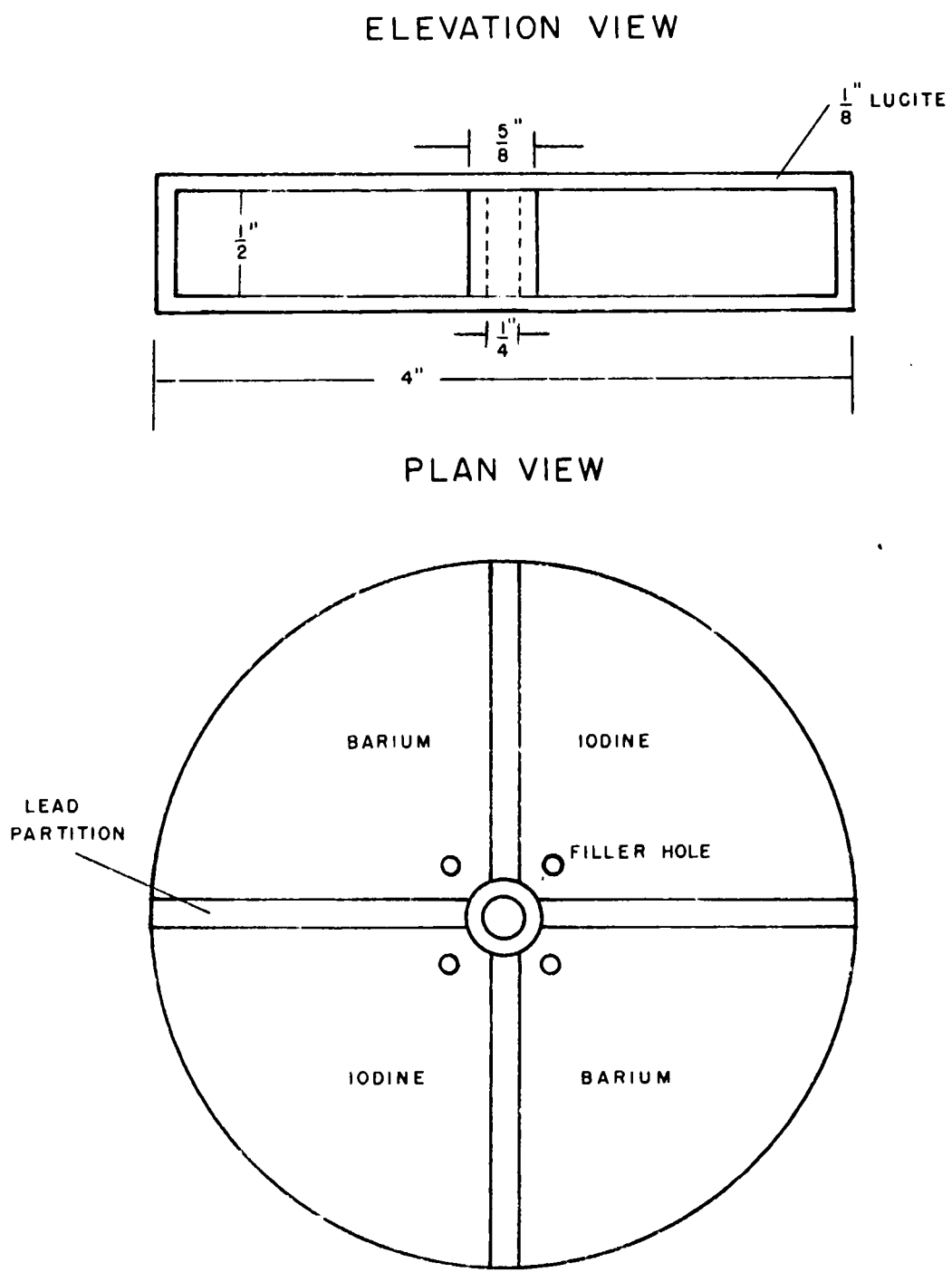

FIG. 6 FILTER CONSTRUCTION DIAGRAM

nated most of the high energy beam as well as the unmodified scatter. The concentration of barium in the second segment, approximately 200 milligrams/cm^2, was chosen such that the intensity of the beam through both filter sections was equal.

Figure 6 is a detail drawing showing the filter construction. The entire assembly is made of lucite with lead partitions. The container has four compartments into which a solution of iodine and barium are introduced. An attempt was made to construct a solid rather than a liquid filter, however, this proved unsuccessful. In order to provide the two monochromatic beams in a serial rather than a parallel fashion the filter is rotated by a synchronous motor at a rate of 1800 revolutions per minute. This means that first the iodine segment then the barium segment is in the secondary beam for a period of 0.083 seconds. The filtered beam is then directed on the iodine sample.

The amount of the secondary beam which is not absorbed by the sample is detected by means of a scintillation probe and the pulses from the probe are then analyzed by a pulse height analyzer. Although most of the features of the pulse height analyzer were used in the experimental stage, it was found that a linear amplifier with a gain of 8000 and a discriminator are all that is necessary.

Both the probe and the analyzer are instruments which are commercially available, in this case both are Picker X-ray Corp. instruments, Model 2970. The crystal used in the scintillation probe is a 1 inch diameter, 2 millimeter thick, sodium iodide crystal which has

extremely good detection efficiencies at the energies used here.

The probe and pulse height analyzer are described in Picker Nuclear Manual No. 12970, however, a list of some of the specifications is in order:

Gain	-- Maximum- 8000, Minimum- 62.5
Rise Time	-- 0.2 microseconds minimum
Clipping Time	-- input clipping time- 2 microseconds amplifier clipping time- 1 microsecond
Linearity	-- 0.6% for the whole system
Resolving Time	-- counting rates of up to 120,000 counts per minute will introduce no distortion in the spectrum
Output	-- 1 volt negative

The pulses which have been analyzed are now fed in serial form to a switch, which channels the train of pulses into two separate counting circuits. This switch is necessary in order to separate the I_{a2} and $I_{a1} + I_{a2}$ beams. This separation process is accomplished with a single pole double throw 60 c/s Bristol chopper No. 95908-10. The chopper has a total dwell time of 0.015 seconds and a transit time of 0.001 seconds. Electronic switches were carefully considered, however, for this application it was found that they added unnecessary complications in the form of triggering circuits and pedestal removing circuits. The electro-mechanical method of switching was found to be by far the simplest and most reliable.

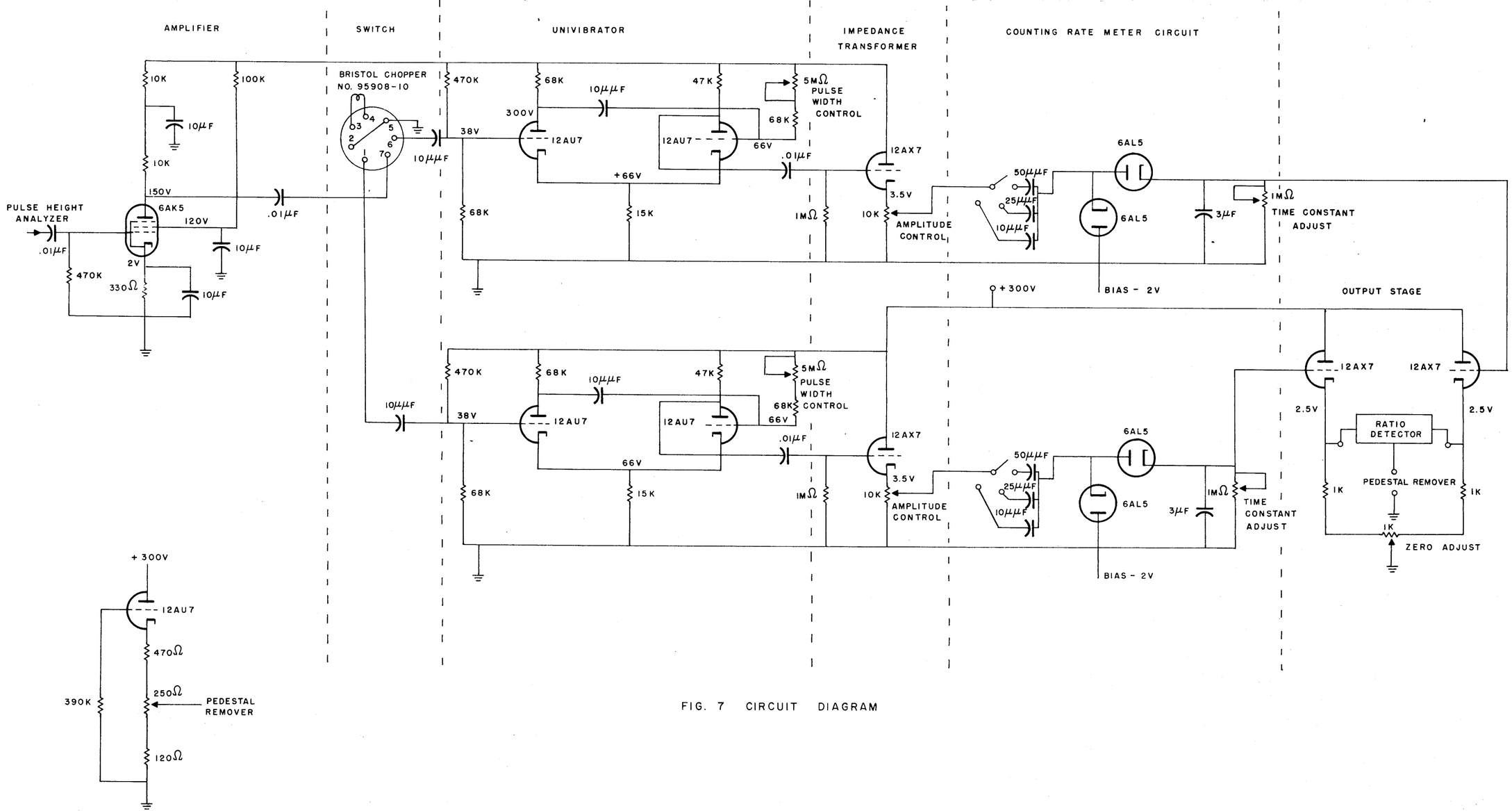

FIG. 7 CIRCUIT DIAGRAM

Synchronization between the chopper and the rotating filter is obtained easily. Since the chopper and synchronous motor are locked together at line frequency, moving the filter container with respect to the motor shaft brings the filter segments into step with the chopper. All that is necessary to synchronize the system is an oscilloscope. Since the filter container has lead partitions there are periodic gaps in the train of pulses coming from the pulse height analyzer. When these gaps no longer appear in the separate channels after the switch, synchronization is completed.

The pulses after being properly switched are counted in two separated circuits and the ratio of these counts is taken. Both the counting circuits and the ratio detector will be described in the next section.

CIRCUIT THEORY

COUNTING CIRCUIT

As shown in the circuit diagram, figure 7, the counting circuit consists of one stage of amplification, a univibrator stage, a cathode follower and an integrating circuit.

1. Amplifier

A single stage of amplification is necessary because the pulse height analyzer produces pulses of insufficient amplitude to trigger the univibrator. The common type of resistance coupled amplifier was chosen and a high frequency pentode tube, 6AK5, was used.

From the equivalent high frequency circuit figure 8, if

$rp \gg R_1$ and $R_2 \gg R_1$

where rp = plate resistance

R_1 = load resistance

R_2 = grid resistance of following stage

C_O = output capacitance

C_1 = input capacitance of following stage

C_H = chopper capacitance each terminal to ground

A_H = high frequency gain

A_M = mid band gain

gm = transconductance

Then $E_{out} = \frac{gm\ E_{IN} R_1}{JwC_S R_1 + 1}$ $\qquad C_S = C_O + C_1 + C_H$

or $\left| \frac{A_H}{A_M} \right| = \frac{1}{\sqrt{1 + (wC_S R_1)^2}}$

$A_H = 46$

Transient Response -- from figure 8

$$I_1 + I_S = gm\ E_I$$

$$\frac{e_o}{R_1} + C_S \frac{de_o}{dt} = gm\ E_I$$

Solving this differential equation gives

$$e = gm\ E_I R_1 \left[1 - \exp - \frac{t}{R_1 C_S} \right]$$

this we see is an exponential build up and the response time from 10 to

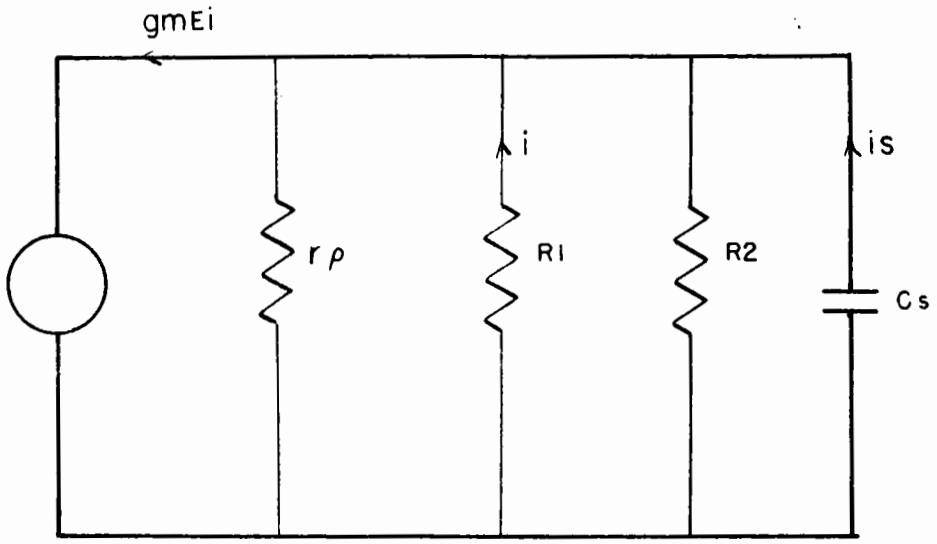

FIG. 8 EQUIVALENT HIGH FREQUENCY DIAGRAM

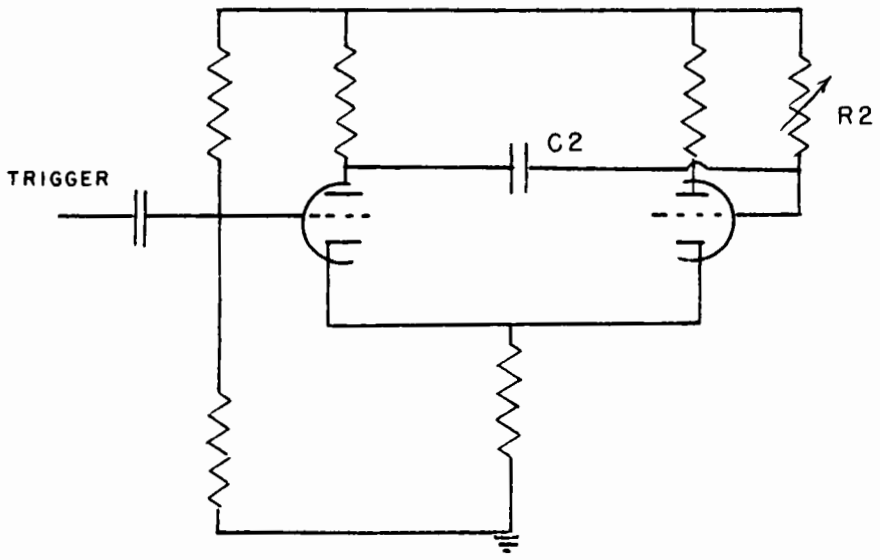

FIG. 9 CATHODE COUPLED UNIVIBRATOR

90 percent is = 2.2 R_1C_S

in our case = 0.19 microseconds

The rise time of the pulse height analyzer is 0.2 microseconds. Therefore no high frequency compensation is necessary.

2. Univibrator

In order to make the counting circuit completely independent of pulse size and shape obtained from the probe and analyzer, a univibrator is used as a pulse shaper. A cathode coupled univibrator was chosen and the design procedure is described (Reintjes et al 1952, p.99) in most standard electrical engineering text books.

Figure 9 shows a schematic diagram of the cathode coupled univibrator. The duration of the quasi-stable state is determined by the time constant R_2C_2. With the components in figure 7 the duration of the pulses is given by

$$t = 0.37\ R_2C_2.$$

Since R_2 is a 5 megohm potentiometer the pulse duration can be varied from 18 microseconds to 1 microsecond. The rise time of the pulses is less than 0.2 microseconds and the amplitude of pulses is 200 volts. The triggering pulse is coupled through a small capacitance to the grid of the non-conducting tube; a positive pulse of at least 12 volts is required to trigger the circuit.

3. Cathode Follower

The cathode follower is used strictly as an impedance transformer, since the integrating circuit requires a source of low impedance

as will be shown later. A 12AX7 triode is used with a 10 kilohm cathode resistance and a megohm grid resistance tied directly to ground. Since all the pulses from the univibrator are positive no additional grid bias is necessary, i.e. batteries or tapping the cathode voltage.

The gain of a cathode follower is given by

$$A = \frac{U}{U + 1} \cong 1 \quad \text{(Reintjes et al 1952, p.64)}$$

Output impedance $Z_o = \frac{rp}{U + 1} \cong 600$ ohms

4. Integrating Circuit

The mechanism by which the integrating or counting rate meter circuit works is very simple (Smith 1952, Williamson 1956, Elmor et al 1949, p.202, Evans 1955, p.803). Each incoming pulse places a definite charge on a capacitor, in a time short compared with the average spacing of pulses. The charge on the capacitor leaks off through a high resistance, making the average potential across the capacitor proportional to the counting rate.

Assuming the following inequalities hold for the circuit shown in figure 10

$$\frac{1}{n} \gg T > 5 R_1 C_1$$

$$E \gg V > E_B$$

$$C_2 \gg C_1$$

where n is the counting rate. In view of these inequalities a charge

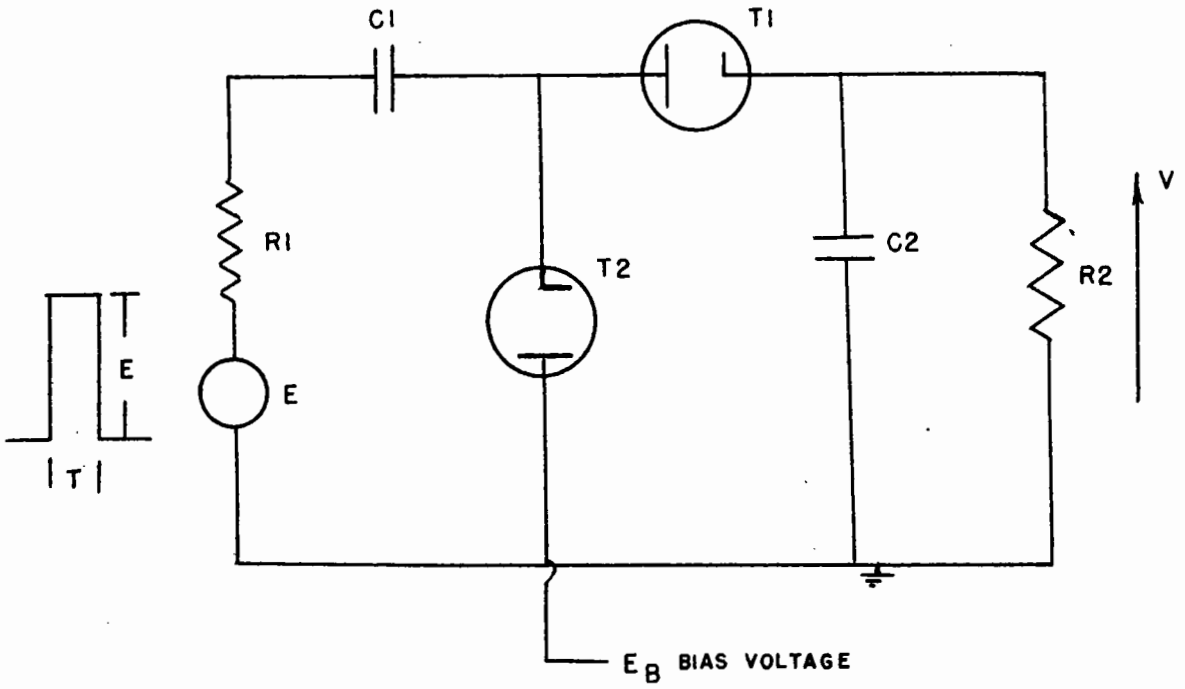

FIG. 10 COUNTING RATE METER CIRCUIT

$q = C_1E$ is deposited on the capacitance C_2 each time a pulse occurs. The average potential V developed across the output terminals is

$$V = n\,q\,R_2 = n\,C_1\,E\,R_2$$

This equation indicates that various ranges of counting rate can be obtained by varying either C_1, R_2, or pulse height E. The small bias placed on the plate of the diode T_2 is necessary to keep the scale linear over the entire range of output voltage. If this bias is not present, a small current may flow through the diodes as a result of differences in contact potential and finite velocity of electron emission from the cathodes of the diodes.

The fractional standard deviation in observed counting rate due to statistical fluctuations in the occurrence of random pulses is

$$S = \frac{1}{\sqrt{2nR_2C_2}} \qquad \text{(Evans 1955, p. 805)}$$

Equilibrium time of the counting rate meter is defined as the time taken for the charge to build up on the capacitor to such a value that it differs from the average value by less than one probable error.

Thus $$t = R_2C_2(0.392 + \tfrac{1}{2} \ln 2nR_2C_2) \qquad \text{(Evans 1955, p. 808)}$$

With the value of components shown in figure 7 the fractional probable error on the highest counting range (5000 c/s full scale) is

$E = 0.5\%$

Equilibrium Time = 10 seconds.

The scale ranges are changed by switching in different values of capacitor C_1; fine adjustment of full scale is achieved by varying the pulse height from the univibrator. R_2 is made variable to equalize

the time constants of both channels thus enabling discontinuities to be seen.

5. Ratio Detector

The ratio of counts is obtained by means of a self-balancing potentiometer. The self-balancing potentiometer, in this case a Systron Model 10 Analog Recorder, compares two voltages and brings the difference between the two to zero. The recorder has a high gain amplifier (approximate gain = 330,000) which drives a two-phase servo motor. The servo is mechanically coupled to a slide wire potentiometer.

Figure 11 is a schematic diagram of the ratio detector. From this diagram it is seen that the ratio of two voltages E_1 and E_2 is given directly by the position of the slider arm,

$$\text{i.e. } \frac{E_1 R_1}{R_T} = E_2 \text{ at null}$$

$$\text{or} \quad \frac{E_2}{E_1} = \frac{R1}{R_T} \qquad 2.1$$

The Systron Recorder has a three turn 5000 ohm potentiometer, full span on the chart is 1.5 turns or 2500 ohms; the source impedance according to the recorder specifications should not exceed 10,000 ohms. Thus in order to couple the counting circuit to the ratio detector an impedance matching device must be used.

Figure 12 shows the circuit diagram of the ratio detector. Two cathode followers are used to couple each counting circuit to the ratio

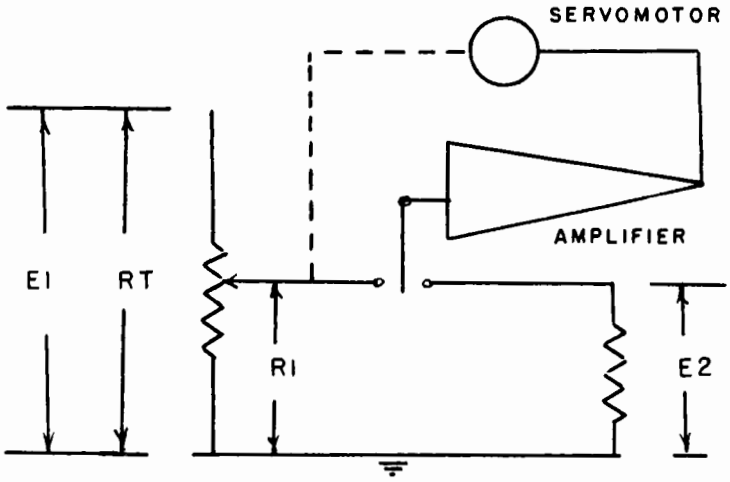

FIG. 11 SCHEMATIC DIAGRAM OF RATIO DETECTOR

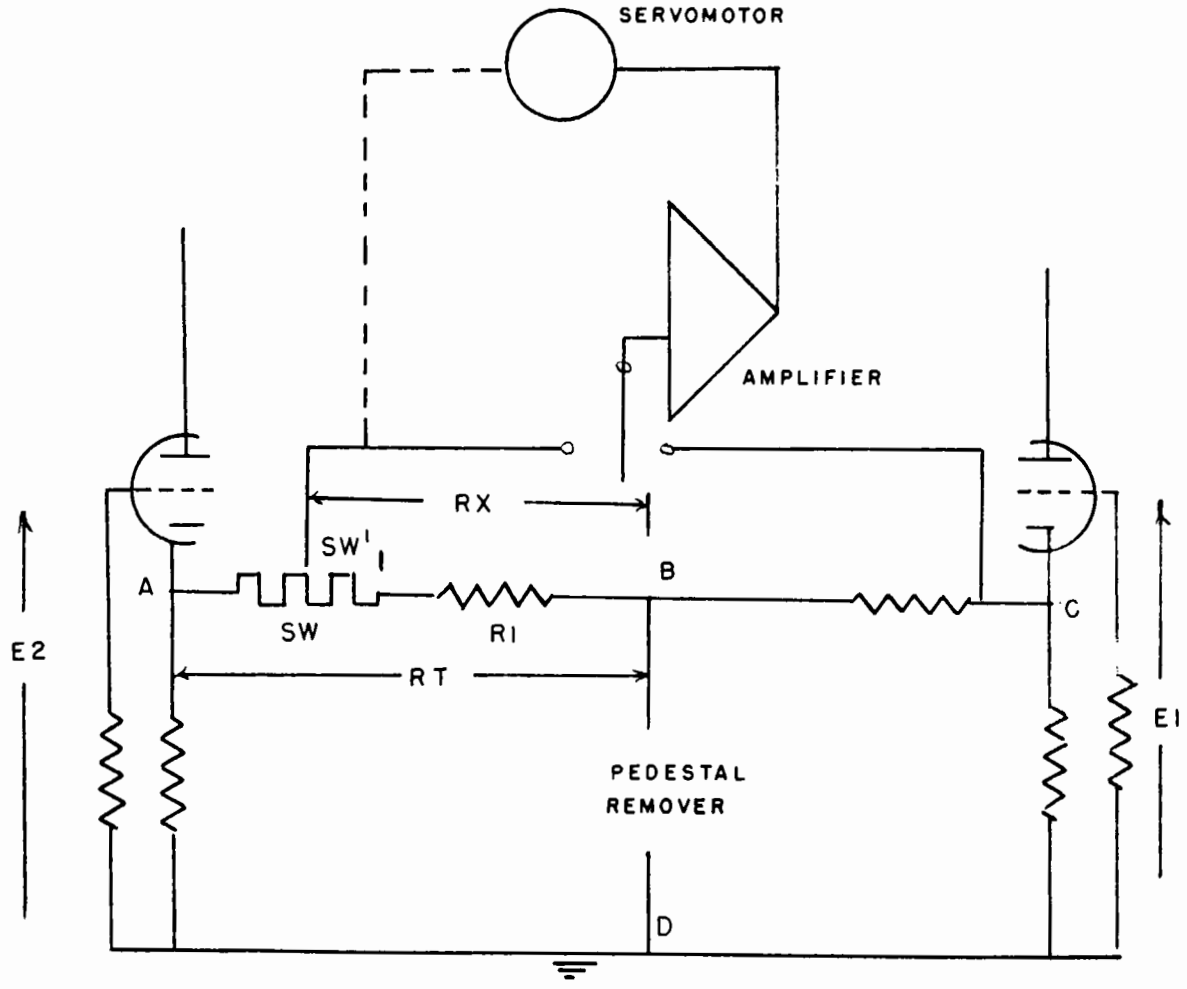

FIG. 12 RATIO DETECTOR

detector. Since each of the cathode followers has a pedestal voltage, i.e. a quiescent voltage with zero input signal, a pedestal remover must be incorporated such that the voltage drop across AB and CB is zero with no input signal,

therefore $V_{AB} = V_{AD} - V_{BD} = E_2$

and $V_{CB} = V_{CD} - V_{BD} = E_1$

hence we get our ratio according to equation 2.1.

If the slide wire SW is the total resistance across AB then the ratio would go from 0 to 1 or 1 to infinity. Since we are interested in very small changes in ratio a scale expansion must be provided. This is very readily accomplished with the addition of resistor R_1. If for instance we would like to have full scale deflection for a change in ratio from 1.0 to 0.9 or say b

$$\text{then } \frac{E_2}{E_1} = \frac{R_X}{R_T} = \frac{R_1 + SW'}{R_1 + SW}$$

for a ratio = 1, SW' =SW, i.e. the potentiometer is at its maximum travel in one direction. For the other limit b, resistance SW' = 0, i.e. it is at the other extreme of its travel.

$$\text{Hence } R_1 = b(R_1 + SW)$$

$$R_1 = \frac{SW}{1 - b}$$

Thus if R_1 is a potentiometer, a scale expansion between 1 and any lower limit can be obtained. Ratio expansion between a and b or say 0.4 and 0.5 can easily be obtained by adding another resistance on the cathode side of the slide wire.

The pedestal remover can either be a battery or, as in this case, another cathode follower. A cathode follower was chosen in order to minimize drift caused by power supply changes, i.e. with a change in power supply voltage all three followers will drift in the same direction producing no effect on the ratio detector. Power supply voltage was varied from 250 to 320 volts with less than a 1% change in ratio.

6. System Drift

The entire system up to the final stage is A.C. coupled, hence drift can only occur in the final cathode follower output stage. If the cathode followers drift by an amount dq_1 and dq_2, then

$$\frac{(E_2 \pm dq_2)}{(E_1 \pm dq_1)} = \text{ratio}$$

$$\text{or} \quad \frac{E_2\,(1 \pm dq_2/E_2)}{E_1\,(1 \pm dq_1/E_1)} = \text{ratio.}$$

Thus we see that the voltage from the counting rate meter circuit should be as large as linearity will allow.

By power series expansion, for small values of $\frac{dq_2}{E_2}$ and $\frac{dq_1}{E_1}$

$$\text{Ratio} \simeq \frac{E_2}{E_1}\left[1 \pm \frac{dq_2}{E_2} \mp \frac{dq_1}{E_1}\right]$$

From this we see that if the drift in the cathode followers is the same the ratio is not effected.

CHAPTER III

PERFORMANCE

An evaluation of the system performance will be made. Figures 13-15 inclusive will show the results of the tests conducted on the electronic circuit alone, while figures 16-23 inclusive will outline the results obtained by testing the lanthanum system with the experimental set-up as shown in the block diagram, figure 5. The results shown in figures 16-23 inclusive were read directly from the chart recorder of the ratio detector during experimentation.

Figure 13 is a calibration curve of the counting rate meter. A variable frequency pulser was used to trigger the univibrator and the voltage across the tank condenser of the counting rate meter circuit was measured. The curve is identical for both counting channels and for all three ranges. The ranges are selected by switching different values of coupling capacitors into the counting circuit. An upper limit of 10,000 c/s total or 5000 c/s per channel was set because the scintillation probe was found to saturate at approximately 15,000 c/s.

Full scale non-linearity of the counting rate meters is ten percent. This however is not detrimental, provided that both channels are identical and operating in approximately the same region.

Figure 14 is a plot of the ratio shown on the recorder when two equal D.C. voltages are applied to the grids of the output cathode followers. As shown the ratio detector works well provided the voltages do not drop below 0.3 volts. Below this point the recorder

amplifier has insufficient power gain, consequently a wide dead span results, and inconsistent results are obtained. A visual check of counting rate is provided by a calibrated microammeter (0-25 microamps) connected between each cathode of the output stage and the pedestal remover. Thus if the counts per second should be such as to produce a voltage less than 0.3 volts the range can be changed or the X-ray output increased.

Figure 15 shows the change in ratio (read directly from the recorder) which occurs when equal counts are applied to both channels and the number of counts varied over the entire counting range. As shown the change in ratio is less than 0.4 percent for any one of the three ranges.

It was found that for a period extending over two hours there was no noticeable drift in the system and with power supply voltage variations of 25 percent there was less than a 1 percent change in ratio.

The system is independent of X-ray voltage and current provided that the voltage is sufficient to excite secondary radiation. Long time drift in the X-ray primary beam does not effect the system inasmuch as a ratio is taken once every 1/60 of a second, i.e. the total sampling time of the chopper.

Figure 16 is the energy spectrum of the lanthanum converter. The system resolution R is defined as the ratio of the width of the peak at half maximum to the energy of the peak mid-point, expressed in percent. The resolution for lanthanum energy at 33 Kev is 35 percent,

for lead at 74 Kev 28 percent, for radioactive gold 198 at 410 Kev 21 percent. Although the system resolution is not fine enough at 33 Kev to resolve the I_{a2} and $I_{a1} + I_{a2}$ beams, the energy spectrum does show that a pulse height analyzer is not necessary since the lanthanum produces no radiation above about 60 Kev. Therefore a linear amplifier and lower level discriminator are all that is necessary. The slight increase at the low energy end of the spectrum is caused by amplifier and detector noise.

Figures 17 and 18 are the attenuation curves of masonite (soft tissue analog) and aluminum (bone analog) respectively. These curves are taken from the actual records, figures 20 and 21. Both the aluminum and the masonite attenuation curves indicate a decrease in ratio while figure 19, the iodine attenuation curve, indicates an increase. This can be explained by referring to figure 4; since iodine has an absorption edge the high energy beam is attenuated more than the low energy beam, whereas in the case of aluminum and masonite the reverse is true. Consequently the ratio in one case is increasing and in the other decreasing.

Figure 19 is a calibration curve of iodine attenuation; values for this curve were taken from the actual record, figure 21. Despite the statistical variations the calibration curve can be easily interpreted as a straight line, thus indicating that equation 1.9 is a good approximation. The change in ratio is less than theoretically predicted: theoretical slope 0.017 per milligram of iodine, actual 0.007 per milligram of iodine. This would indicate that the values

for U_1, U_2 and K chosen for the theoretical slope term are rough approximations. There are techniques available to measure these values, however, for the present it was felt that this was unnecessary.

It is evident from the actual records of the masonite and aluminum absorption curves that an attempt to determine the amount of each of these substances that causes the same change in ratio as 1 milligram of iodine, will be a rough estimate at best. Nevertheless from figure 17 we see that by increasing the masonite from 2 to 4 cm., or by 2000 milligrams/cm^2, causes a change in ratio of 0.7 percent or the same as 1 mg./cm^2 of iodine. From figure 18 we see that 4 mm of aluminum or approximately 1000 milligrams/cm^2 also causes a 0.7 percent change in ratio.

Figure 23 shows that this method of iodine determination is truly feasible in that iodine can be detected even in the presence of foreign elements and that the ratio is independent of the amount of foreign substance introduced into the secondary beam.

Although all the preceding tests were carried out in vitro, the results indicate that in vivo iodine determination is highly practicable with this lanthanum system. Future tests in vivo are planned which should prove the worthiness of this method.

TABLE III

VALUES FOR COUNTING RATE METER CALIBRATION CURVE

RANGE 1		RANGE 2		RANGE 3	
Counts/sec	Voltage	Counts/sec	Voltage	Counts/sec	Voltage
100	0.52	100	0.28	250	0.27
150	0.76	200	0.53	500	0.52
200	1.01	300	0.78	750	0.76
250	1.25	400	1.03	1000	1.00
300	1.50	500	1.28	1250	1.26
350	1.75	600	1.50	1500	1.49
400	1.99	700	1.73	1750	1.73
450	2.22	800	1.96	2000	1.98
500	2.45	900	2.18	2250	2.19
550	2.68	1000	2.45	2500	2.43
600	2.90	1100	2.64	2750	2.64
650	3.18	1200	2.87	3000	2.90
700	3.41	1300	3.15	3250	3.18
750	3.65	1400	3.38	3500	3.41
800	3.80	1500	3.60	3750	3.62
850	4.05	1600	3.80	4000	3.80
900	4.20	1700	4.00	4250	4.00
950	4.39	1800	4.15	4500	4.18
1000	4.59	1900	4.35	4750	4.37
		2000	4.54	5000	4.55

FIG. 13 COUNTING RATE METER CALIBRATION CURVE

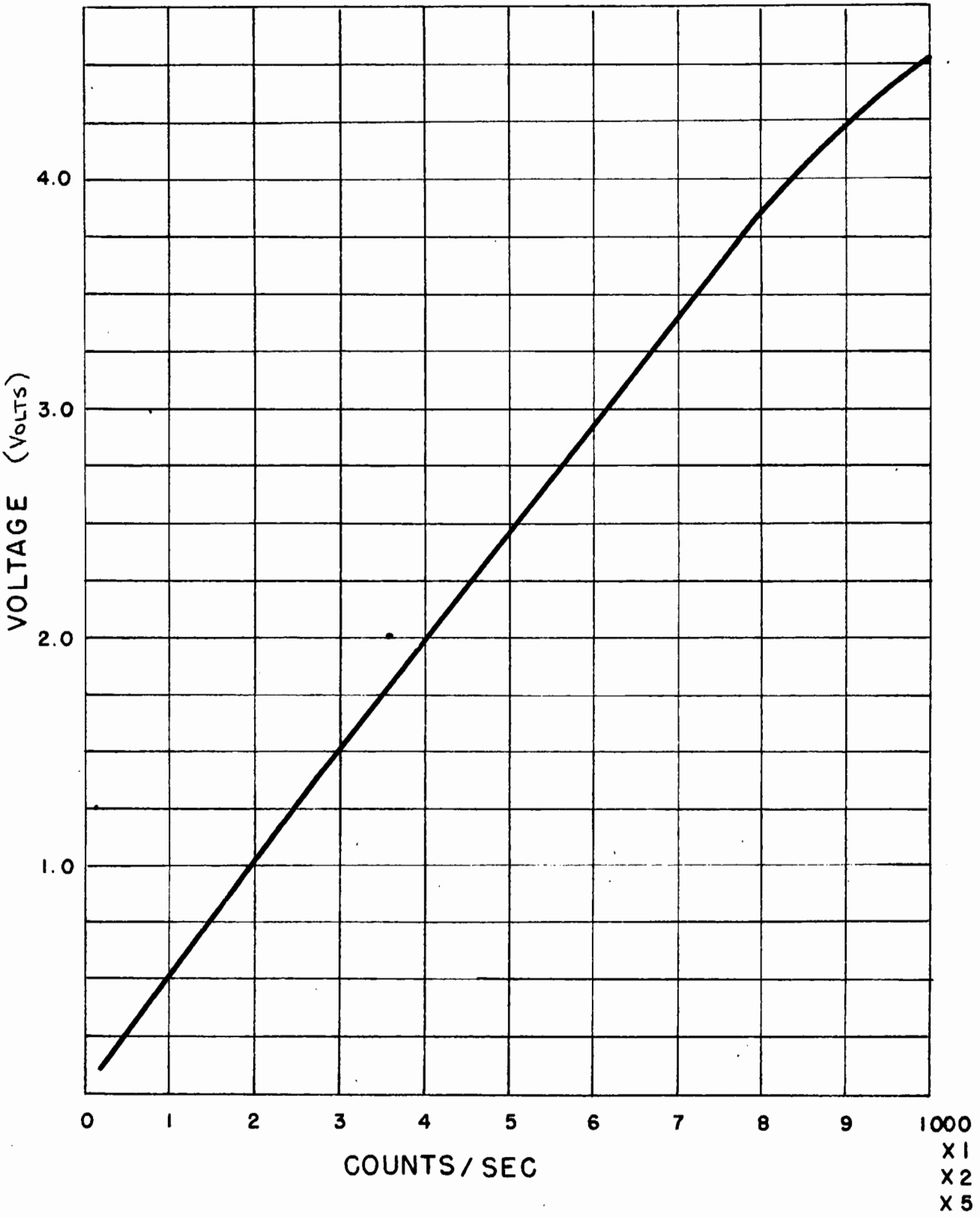

FIG. 14 RATIO VARIATION WITH D.C. VOLTAGE

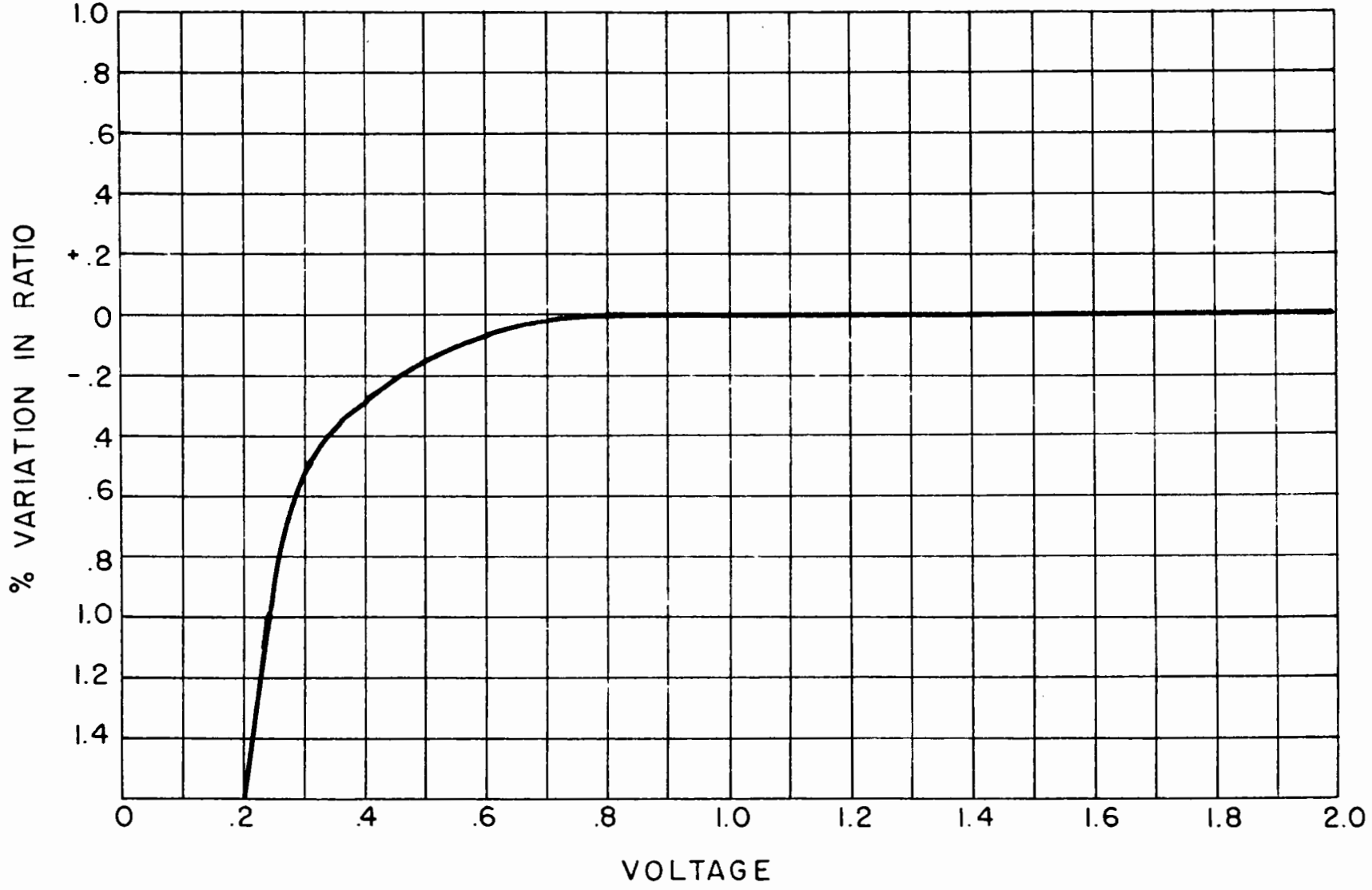

FIG. 15 RATIO VARIATION WITH COUNTING RATE

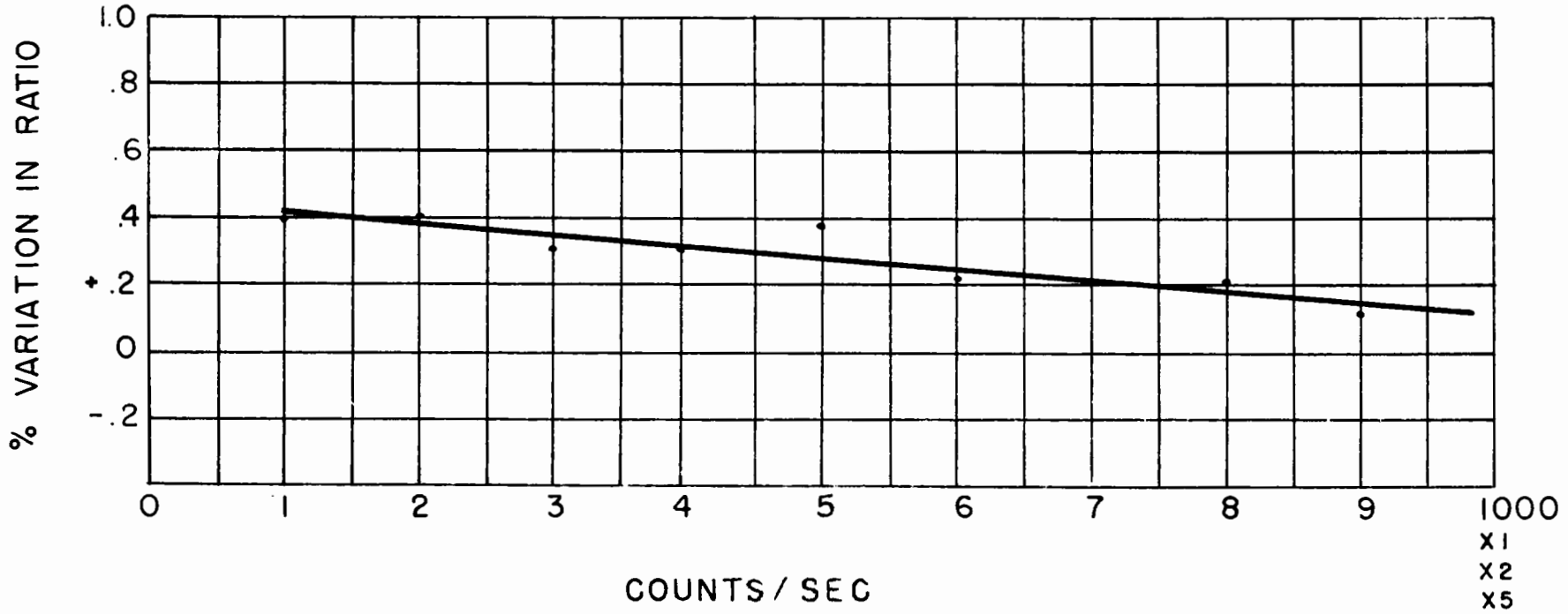

FIG. 16 LANTHANUM CONVERTER ENERGY SPECTRUM

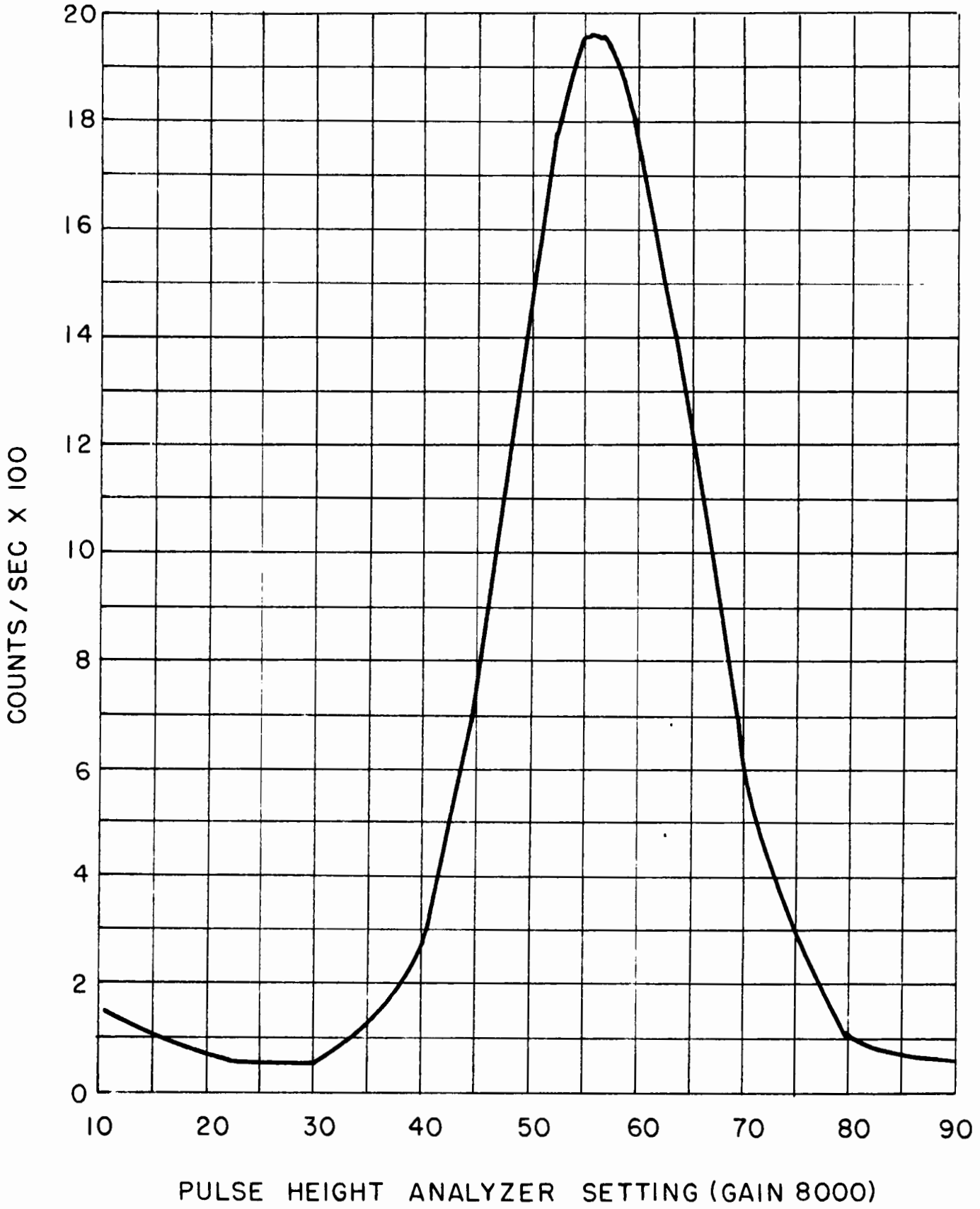

FIG. 17 MASONITE ATTENUATION CURVE

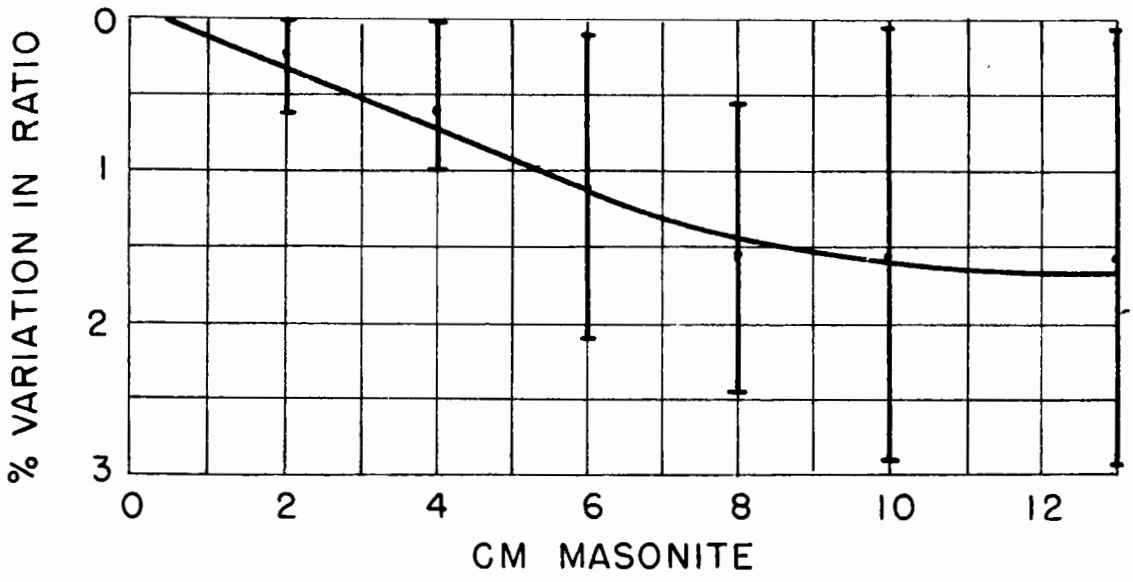

ERROR = 95% CONFIDENCE

FIG. 18 ALUMINUM ATTENUATION CURVE

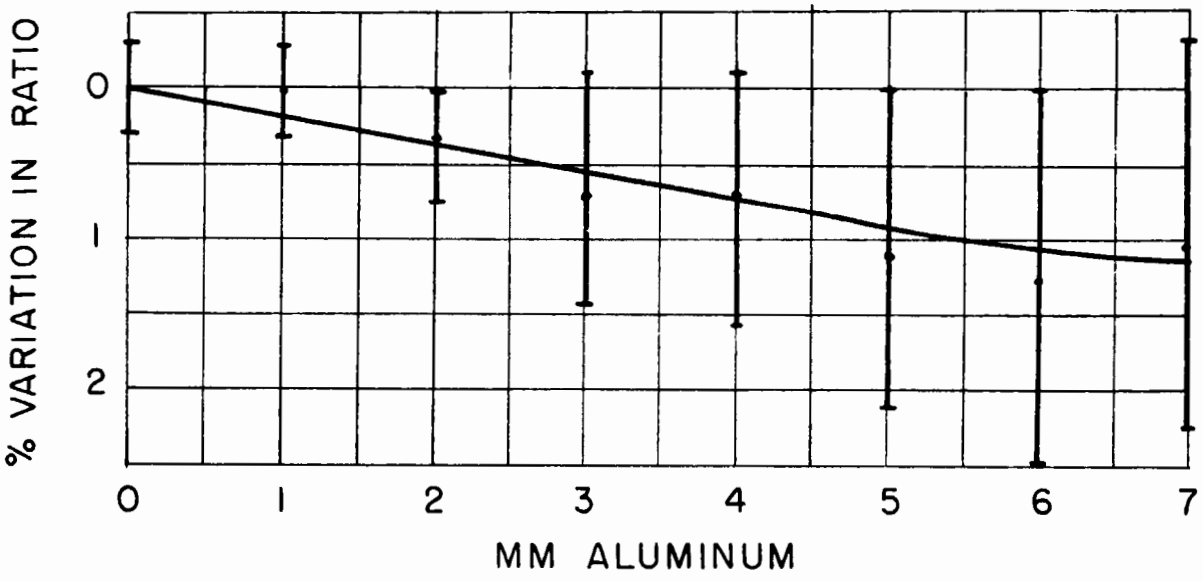

ERROR = 95% CONFIDENCE

FIG. 19 IODINE ATTENUATION CURVE

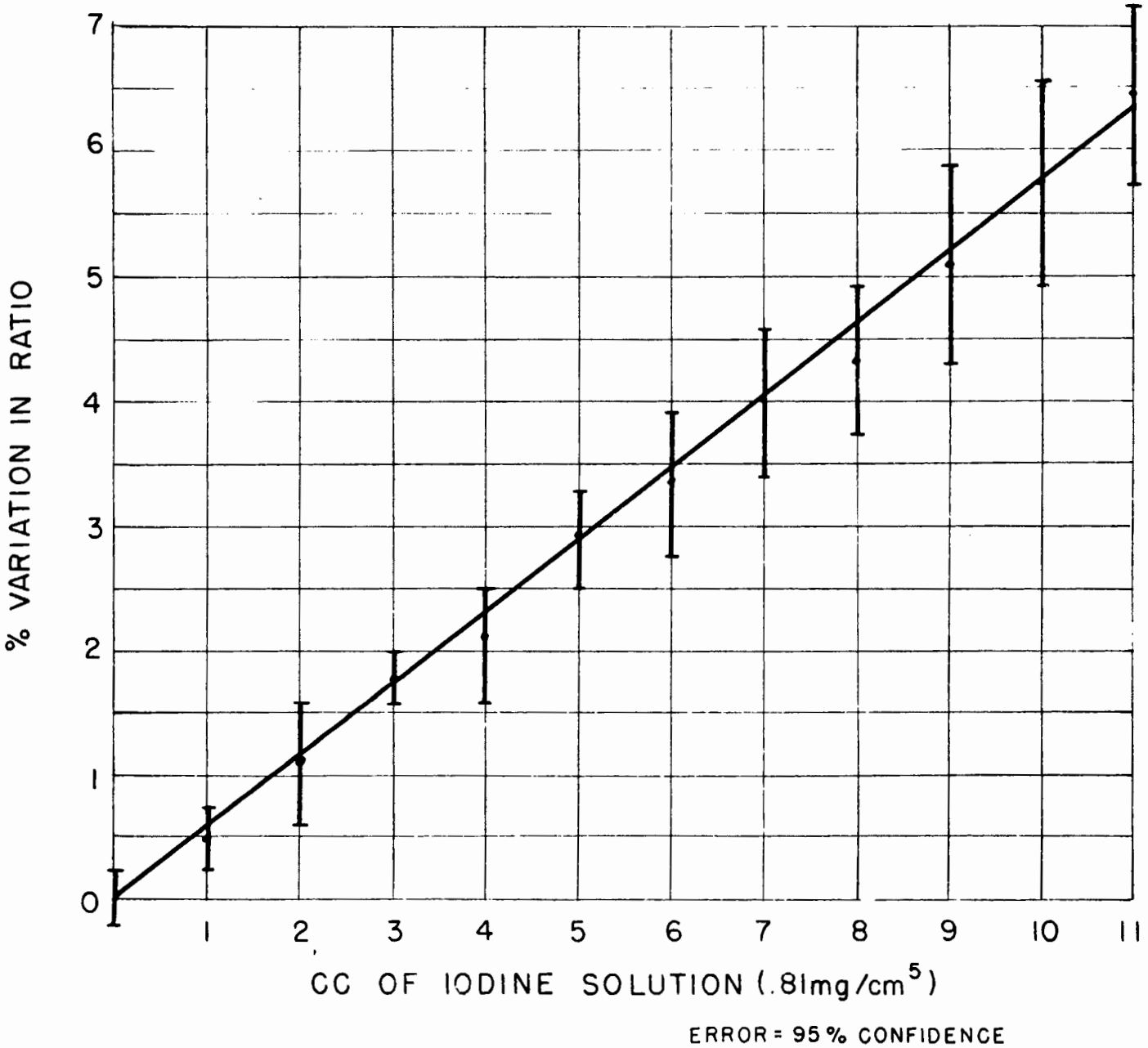

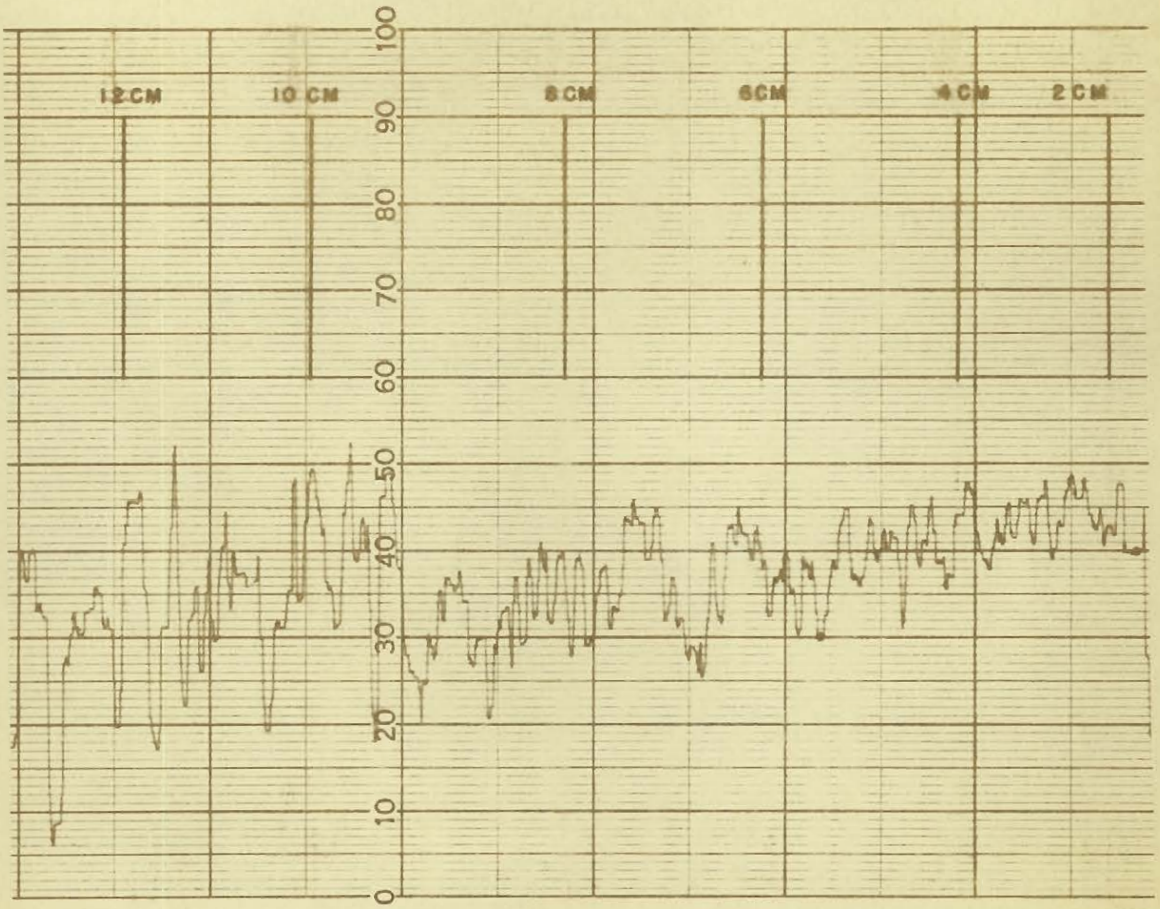

FIG. 20 MASONITE ATTENUATION CURVE

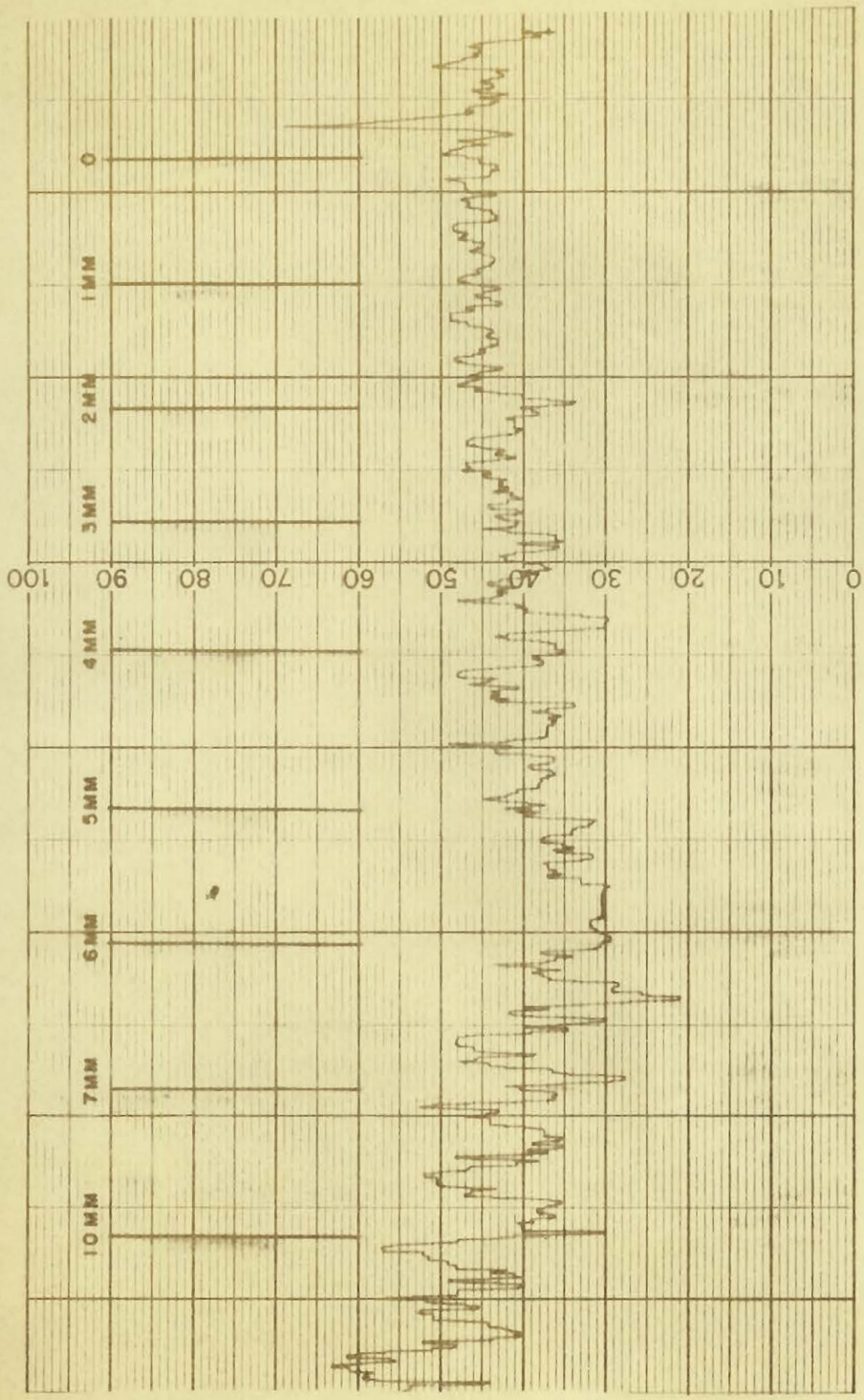

FIG. 21 ALUMINUM ATTENUATION CURVE

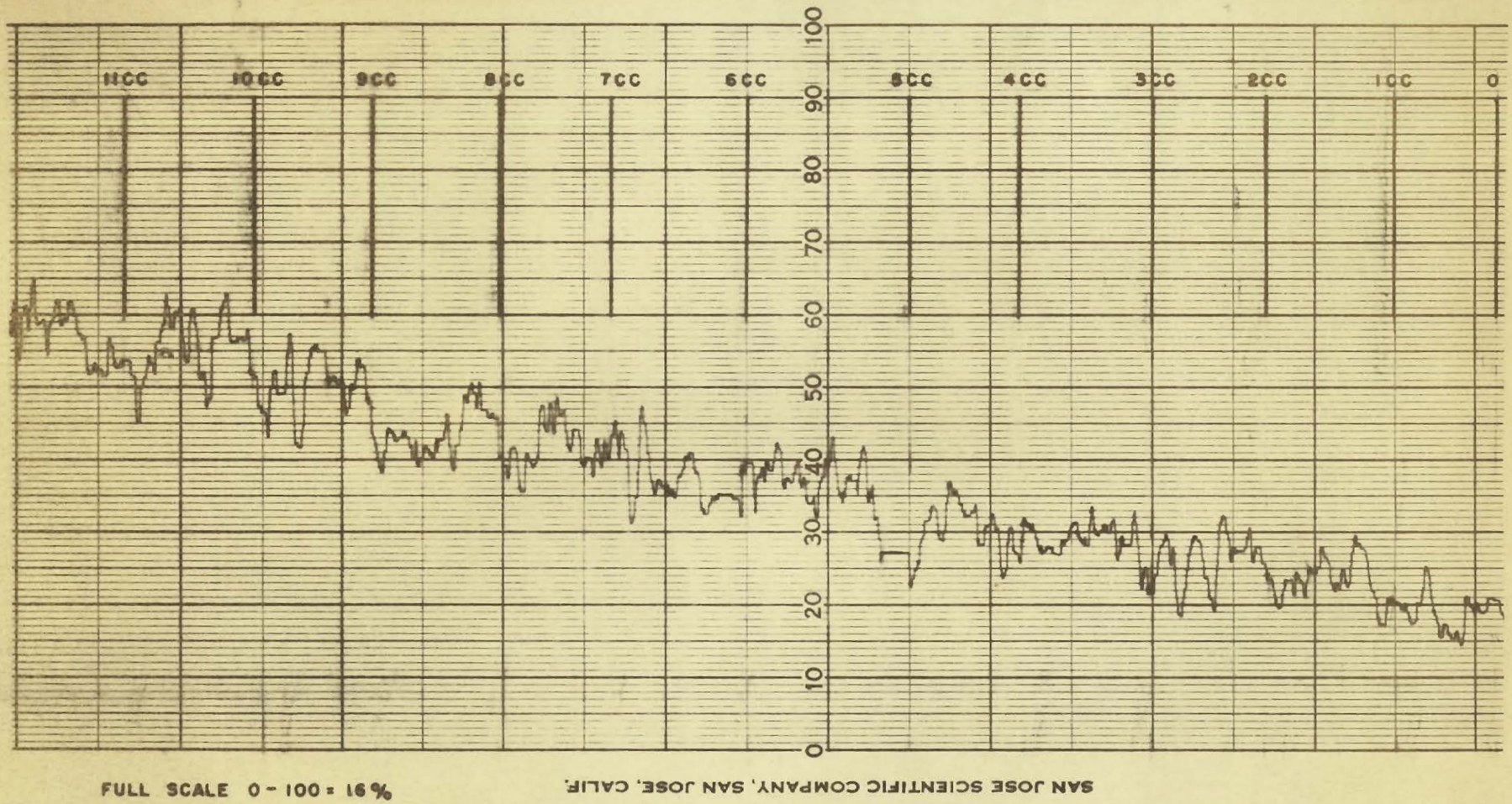

FIG. 22 IODINE ATTENUATION CURVE (0.81mg/cm^5)

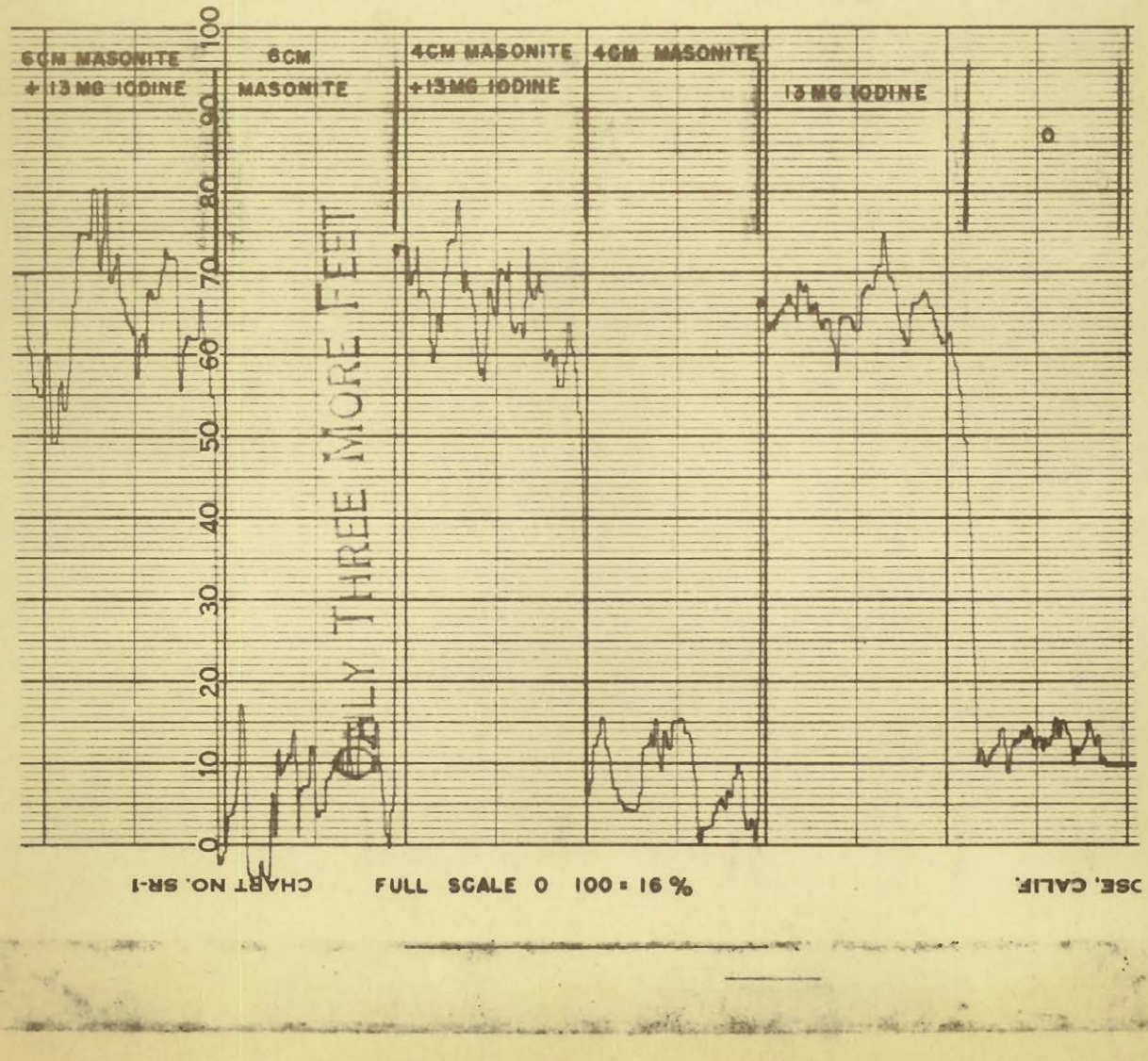

FIG. 23 EFFECT OF MASONITE ON IODINE DETERMINATION

SUGGESTIONS

Statistical fluctuations may be a source of irritation to an untrained eye. Since radiologists are trained in viewing contrast media, such as film, an output other than a chart type could be used. One method is to photograph the face of a cathode ray tube whose beam intensity has been modulated by the ratio voltage; another is to vary the light output of a neon bulb and record the intensity changes on photographic film. Perhaps a presentation in the form of a hystogram may be more desirable. This can be obtained by using two scalers and taking the ratio once every second or over any other period of time.

An increase in secondary radiation would be desirable to decrease the statistical fluctuations when iodine is to be detected in the presence of a large amount of foreign elements. With a single stationary converter system, the target in the X-ray tube itself could conceivably be made of a substance such as lanthanum sulphide. Thus the intensity of secondary radiation would be increased greatly over the present system.

It has been stated in the text that the probe saturates at approximately 15,000 c/s; this is due chiefly to the many pulses which occur in very short bursts. It is felt that the range of the probe can be extended by using a constant potential machine, thus obtaining a more uniform distribution of pulses.

APPENDIX I

The fraction of radiation absorbed in passing through a thin layer of matter is proportional to the thickness x of the layer and a factor called the "linear attenuation coefficient" which depends upon the nature of the absorbing matter and the energy of radiation.

Throughout the thesis U has been designated as the "mass attenuation coefficient" and this is equal to the linear attenuation coefficient divided by the density of the substance. The mass absorption coefficient was used because it is characteristic of the absorbing substance whereas the linear coefficient is not. Thus the linear attenuation coefficient for a given beam of X-rays is much greater in water than in steam whereas the mass attenuation coefficient is the same in both, because in the case of mass absorption it does not matter whether the X-rays traverse one gram of water or one gram of steam the result will be the same, i.e. independent of density. The units for the mass attenuation coefficients are $\frac{cm^2}{gm}$. In order to make the exponent term of equation 1.1 unitless the concentration x is expressed in gms/cm^2.

BIBLIOGRAPHY

deBroglie, M., J. Phys., 5, p. 227 (1916).

Fine, S. and Hendee, C.F., "X-ray Critical Absorption and Emission Energies in Kev", Nucleonics, Vol. 13, No. 3, p. 36 (March 1955).

Glocker, R. and Frohnmayer, W., Ann Physik, 4, 76, p. 369 (1925).

Engstrom, A., Cosslett, V.E. and Pattie, H.H., "X-ray Microscopy and Microradiography", Academic Press, New York (1957).

Jacobson, B., "Dichromatic Absorption Radiography Dichromography", Acta Radiologica, Vol. 39, p. 437 (June 1953).

Jacobson, B. and MacKay, R.S., "Advance in Biological and Medical Physics", Academic Press, New York, Vol. 6, p. 201 (1958).

Compton, A.H. and Allison, S.K., "X-ray in Theory and Experiment", D. Van Nostrand Co., Princeton, New Jersey (1957).

Evans, R.D., "The Atomic Nucleus", McGraw-Hill Co., New York (1955).

Nelms, A.T., "Graphs of the Compton Energy-Angle Relationship and the Klein-Nishina Formula from 10 Kev to 500 Mev", National Bureau of Standards, Circular No. 542, Washington, D.C. (August 28, 1953).

Picker Nuclear, "Pulse Height Analyzer 2970", Picker X-ray Co., White Plains, New York, Manual WP No. 12970.

Reintjes, J.F. and Coate, G.T., "Principles of Radar", McGraw-Hill Co., New York (1952).

Smith, G.S., "Counting-Rate Meters", Electronic Engineering, Vol. 24, p. 14 (January 1952).

Williamson, C.N., "Direct Reading Pulse Counter", Electronics, Vol. 29, No. 12, p. 194 (December 1956).

Elmore, W.C. and Sands, M., "Electronics Experimental Techniques", McGraw-Hill Book Co., New York (1949).